



**TÉCNICO**  
LISBOA

## **Characterizing the Cyclists' Path**

Overtaking Maneuver Detection and Vehicles' Speed Estimation

**Filipa Fernandes Adanjo de Oliveira**

Thesis to obtain the Master of Science Degree in

**Electrical and Computer Engineering**

Supervisors: Dr. Manuel Ricardo de Almeida Rodrigues Marques

Prof. João Paulo Salgado Arriscado Costeira

### **Examination Committee**

Chairperson: Prof. João Fernando Cardoso Silva Sequeira

Supervisor: Dr. Manuel Ricardo de Almeida Rodrigues Marques

Member of the Committee: Prof. João Miguel Raposo Sanches

**July 2018**



## **Declaration**

I declare that this document is an original work of my own authorship and that it fulfills all the requirements of the Code of Conduct and Good Practice of the Universidade de Lisboa.



## **Agradecimentos**

Um grande agradecimento ao meu orientador, Dr. Manuel Ricardo de Almeida Rodrigues Marques, pelo seu interesse genuíno em ajudar, disponibilidade e paciência.



## Resumo

Nos últimos anos, a poluição e os transtornos causados pelo tráfego em áreas urbanas tem vindo a aumentar. Neste sentido, várias medidas têm sido adotadas para publicitar a utilização de meios de transportes mais sustentáveis, como as bicicletas. Para fortalecer esta tendência e projectar novas infra-estruturas surge a necessidade de criar ferramentas que permitam realizar uma avaliação dos trajectos para bicicletas.

Neste projecto, propõe-se um método baseado na avaliação de sequências de imagens de modo a identificar manobras de ultrapassagem realizadas nas proximidades dos ciclistas e estimar a velocidade dos veículos envolvidos. Os dados obtidos forneceram informações importantes que poderão ser utilizadas por planeadores urbanos na caracterização de vias para circulação de bicicletas.

A abordagem escolhida foi testada em imagens capturadas por uma câmara em zonas urbanas distintas. Os resultados obtidos foram promissores, tendo permitido comparar diferentes zonas quanto à caracterização das mesmas para circulação de bicicletas tendo em conta a rapidez com que os veículos ultrapassam os ciclistas.

**Palavras-chave:** Ciclista, Manobra de ultrapassagem, Reconhecimento de matrículas, Rapidez.



## **Abstract**

The traffic pollution is a scourge of urban areas and several transportation policies have been adopted to increase the use of sustainable transportation, such as bicycles. To develop this desirable trend and design new infrastructures, policy makers require tools for cyclists' risk assessment. In this work, a video-based method to estimate overtaking maneuvers and vehicles' speed is proposed. It was possible to geo-reference these stressful events for riders, providing a framework for path characterization concerning roads' suitability and safety for cyclists.

From action camera sequences of images and smartphone's GPS data, the proposed method is based on license plate recognition and tracking of approaching vehicles near cyclist surroundings.

A new dataset with realistic bicycle scenarios in urban roads is made available and used as case of study. It was possible to compare distinct streets and differentiate different urban areas based on the speed of detected overtaking maneuvers.

**Keywords:** Cyclist, Overtaking Manuever, License plate recognition, Vehicle Speed.



# Contents

Acknowledgments . . . . .	v
Resumo . . . . .	vii
Abstract . . . . .	ix
List of Tables . . . . .	xiii
List of Figures . . . . .	xv
Nomenclature . . . . .	xvii
Glossary . . . . .	xxi
<b>1 Introduction</b>	<b>1</b>
1.1 Cyclists Numbers . . . . .	3
1.1.1 Mapping cyclists experience . . . . .	4
1.1.2 Data Acquisition . . . . .	5
1.2 General goals . . . . .	6
1.3 Thesis Outline . . . . .	6
<b>2 Maneuver Identification System</b>	<b>7</b>
2.1 State-of-the-Art . . . . .	7
2.1.1 Vehicle Detection and Tracking . . . . .	7
2.1.2 Vehicle Speed Estimation . . . . .	8
2.1.3 Events Detection . . . . .	8
2.1.4 Previous developments . . . . .	9
2.1.5 License Plate Recognition . . . . .	9
<b>3 Proposed Approach</b>	<b>11</b>
3.1 Data Set . . . . .	12
3.2 Detection . . . . .	12
3.2.1 Outliers . . . . .	15
3.3 Vehicles Tracking . . . . .	15
3.4 Vehicle Speed Estimation . . . . .	18
3.5 Maneuver Identification . . . . .	22
3.6 Mapping . . . . .	24

<b>4 Results</b>	<b>27</b>
4.1 Overtaking Maneuver Identification . . . . .	27
4.2 Speed Estimation Error . . . . .	29
4.3 Application . . . . .	29
4.3.1 Characterization . . . . .	31
<b>5 Conclusions</b>	<b>35</b>
5.1 Conclusions . . . . .	35
5.2 Future Work . . . . .	35
<b>Bibliography</b>	<b>37</b>
<b>A Figures</b>	<b>A.41</b>
A.1 Overtaking Maneuvers Identification . . . . .	A.41
<b>B Tables</b>	<b>B.45</b>
B.1 Streets Characterization . . . . .	B.45

# List of Tables

3.1	License character sequence recognition performance. . . . .	14
3.2	Color range representation for speed intervals . . . . .	24
4.1	Detection results for each type of overtaking maneuver. . . . .	28
4.2	Overtaking maneuvers detections results with area and speed range specification. . . . .	31
4.3	Overtaking maneuvers detections results. Street and speed range specification. . . . .	34
B.1	Bicycle suitability methods, acronym, reference, citation and date. . . . .	B.45
B.2	Side-by-side comparison of considered variables on listed methods. . . . .	B.46
B.3	Specific streets characterization. . . . .	B.47



# List of Figures

1.1	Occurrences mapping based on GPS data and speed estimation for overtaking maneuvers performed near cyclists. . . . .	2
1.2	Reported road casualties in UK . . . . .	3
1.3	Reported road casualties in Portugal . . . . .	4
1.4	System Architecture . . . . .	5
3.1	Implementation process from a vehicle's detection to maneuver identification. . . . .	11
3.2	License Plate Recognition Input and Output representation with OpenAlpr . . . . .	12
3.3	Plate Region Calibration . . . . .	13
3.4	Plate Region Estimation . . . . .	13
3.5	Character Segmentation . . . . .	14
3.6	Other sequence of numbers is identified on the vehicles rare. . . . .	15
3.7	Scheme of the subset of active vehicles . . . . .	18
3.8	Rotation matrices and translation vectors estimation between two detections. . . . .	21
3.9	Representation of distance measurement between two detections . . . . .	22
3.10	Overtaking maneuver example . . . . .	22
3.11	3D Representation of all detections of a vehicle performing an overtaking maneuver. . . . .	23
3.12	Parked vehicle example . . . . .	23
3.13	3D Representation of all detections of a parked vehicle. . . . .	24
3.14	Georeference of overtaking maneuvers detected for a single trip. . . . .	25
4.1	Overtaking zones based on lane division . . . . .	27
4.2	False negatives representation . . . . .	28
4.3	Representation of traveled areas segmented into 7 different zones. . . . .	30
4.4	Representation of all overtaking maneuvers detected in Campo de Ourique. . . . .	31
4.5	Representation of detected overtaking maneuvers in 2 specific streets (Amoreiras) . . . . .	32
4.6	Representation of detected overtaking maneuvers in 2 specific streets (Entrecampos) . . . . .	33
4.7	Representation of all overtaking maneuvers detected in several trips in a specific section of a street (Av. Alm. Reis) . . . . .	33
A.1	Overall representation of distance measurement evaluation between detections for maneuver identification . . . . .	A.41

A.2	3D Representation of all detections of a vehicle performing an overtaking maneuver. . . .	A.42
A.3	3D Representation of all detections to a parked vehicle. . . . .	A.43

# Nomenclature

$A_i$	$2 \times 9$ matrix
$A$	$8 \times 9$ matrix
$C$	Cost matrix
$c_{nm}$	Final cost of associating a new detection $n$ with vehicle $m$
$c_{nmF}$	Cost of associating a new detection $n$ with a tracked vehicle $m$ at frame $F$
$d_{nmF}$	Difference between centroids of licenses $m_F$ and a new detection $n$
$F$	Current frame
$\delta_d$	Threshold value for distance penalization
$\delta_t$	Threshold value for time penalization
$\Delta dist_{(i,j)}^m$	Difference between translation vector of two detections of the same vehicle $m$
$\gamma$	Threshold value for new detections
$\lambda, \alpha$	Scalar factores
$\lambda_{1,2}$	Singular values of $G'$
$K$	Intrinsic camera matrix
$l_{nmF}$	Number of equal letters between a new detection $n$ and a tracked vehicle $m_F$
$m$	Index of detected vehicle
$m_F$	Detection of vehicle $m$ at frame $F$
$G$	Product of the inverse matrix of camera intrinsic parameters $K$ with the homography matrix $H$
$G'$	Two first columns of matrix $G$
$G''$	Last column of $G$
$H$	$3 \times 3$ homography matrix
$h$	Vector of homography matrix entries

$K$	Intrinsic camera matrix
$n$	New detection
$P_i$	Reference plate coordinates
$p_i^{x,y,z}$	3D location of corner $i$
$p^i$	Points in the image of the reference frame
$p^F$	3D location of corner $F$
$q$	2D points $(q^x, q^y)$ in an image
$q'$	2D points $(u, v)$ in an image
$q^{x,y}$	Coordinates of point $q$ ( $x$ and $y$ ) in the image
$q'^{u,v}$	Coordinates of point $q'$ ( $u$ and $v$ ) in the image
$R$	Rotation matrix
$R'$	Two first columns of rotation matrix $R$
$R^m$	Set of all rotation matrices between all elements of a vehicle $m$
$R_{(c_F, l_F)}^m$	Rotation matrix between the camera and a license plate for vehicle $m$
$t$	Translation vector
$t(i, j)^m$	Translation vector between license plates in two different frames of the same vehicle $m$
$t_{(c_F, l_F)}^m$	Translation vector between the camera and a license plate for vehicle $m$ in frame $F$
$r_{i,j}$	Time instance of two detections of the same vehicle, $i$ and $j$
$r_n$	Time instance of a new detection $n$
$r_v$	Time instance of the last detection to a certain vehicle
$r_w$	Time window
$sp^m$	Speed value associated with vehicle $m$
$w_{1,2}$	Weights associated with time and distance measurements
$w_{b_{1,2,3}}$	Weights associated with recent detections
$U$	Unitary matrix
$u_i, v_i$	2D projection of corner $i$
$V$	Left-singular vectors of $G'$
$v_m$	Set with all detections of a vehicle $m$

- $\mathcal{V}$  Set of all tracked vehicles
- $\mathcal{V}^a$  Set of all active tracked vehicles



# Glossary

<b>ASNR</b>	Autoridade Nacional Segurança Rodoviária
<b>BLOS</b>	Bicycle Level of Service
<b>CNNs</b>	Convolutional Neural Networks
<b>FN</b>	False Negative
<b>FP</b>	False Positive
<b>GPS</b>	Global Positioning System
<b>IMU</b>	Inertial Measurement Unit
<b>LBP</b>	Local Binary Patterns
<b>OCR</b>	Optical Character Recognition
<b>ROSPA</b>	The Royal Society for the Prevention of Accidents
<b>SVD</b>	Singular Value Decomposition
<b>SVM</b>	Support Vector Machine
<b>TTS</b>	Time to stop



# Chapter 1

## Introduction

Big city traffic problems have increased in the last years, which led to the need of finding alternative solutions and transportation policies. The seriousness of the situation has led to the search for healthier and less expensive options, such as bicycles. However, the lack of conditions and streets' planning, turns choose a safe route an impossible task. In order to design new infrastructures, new tools for streets characterization and cyclists' risk assessment are required.

In [1, 2] new approaches have been proposed concerning cyclists path characterization, presenting a system able to process image sequences, gather important information and provide specific descriptors to characterize roads and assist cyclists on travel path decision. Based on image processing, Vieira *et al.* [1] proposed an automatic classification of cyclists' maneuvers, like turn right and left, or interactions between cyclists and vehicles. This previous work also shown the correlation between these interactions and stressful events. In [2], a new descriptor to access the route risk from the cyclist perspective was proposed, taking into account the type of obstacles (people, cars, etc.) on the route.

Several methods have been proposed to classify roads suitability regarding bicycles circulation, in [3] and [4]. Lane width, vehicles speed and traffic flow are the most used parameters.

To access bicycle suitability, several methods have been developed over the years. Methods take into account different attributes of the cyclist's environment, ranking to each with a certain number of points. These points are then used to compute a score for the cycle lanes to determine desirability or undesirability and to make comparison between cycle lanes. Which attributes a method uses and what weights each have vary from method to method.

One such example is the Bicycle Level of Service (BLOS), as defined by the High Capacity Manual [5]. Intersections and roads are characterized by giving a value to each relevant attribute, and then combining all with the respective weights as the BLOS score. For example, in the case of a road section without intersections, the relevant attributes are: vehicle traffic volume, vehicle speed and cyclists' operating space.

Besides the BLOS, other metrics have been defined in the literature. According to [6] and [7] some examples of the literature where selected, as presented in Table B.1. A comparison of the variables used in each method can be seen in Table B.3, in which it is possible to highlight vehicle speed in every

bicycle suitability estimation. This being said, vehicle speed and overtaking maneuver occurrences, as evidenced in [8], are very important parameters to take into account for cyclist path's suitability evaluation.

Further, the importance of speed estimation for bicycle suitability assessment is also mentioned in [9] and [10]. The main goal of the presented work is the estimation of vehicle's speed in order to identify overtaking maneuvers performed in the cyclist's surroundings. In order to compute vehicles' proximity with one single camera is necessary to know the dimensions of the objects. Since vehicles' sizes vary, there was the need to choose an object with known dimensions that could be used to identify vehicles. In this sense a new option emerged, using license plates recognition as a tool for vehicles detection.

A new approach to estimate vehicle proximity and speed is proposed based on license plate detection and tracking from data provided by a camera located at the bicycle's handlebar.

Accurately identify overtaking maneuvers occurrences and estimate the corresponding vehicle speed in each specific track section is very important to correctly characterize streets. Therefore, these two modules will be the main focus of the present work. With data gathered from specific streets it will be possible to build a data set based on up to date bicycle data.

This development, together with previous works of [2] and [1], aims to provide a more reliable risk assessment system for street characterization aimed at bicycle circulation. Also in these works, a smartphone application was developed and used to gather data from a smartphone device, which allowed to identify events location and map the occurrences, as illustrated in Fig.1.1.

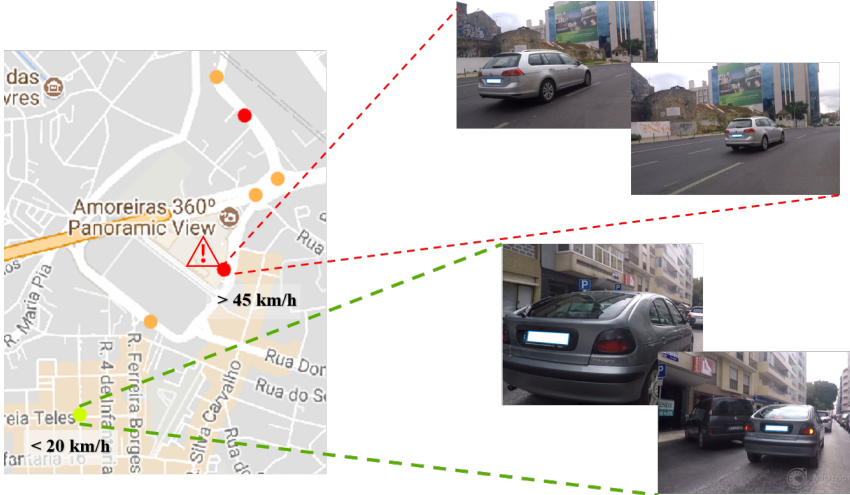


**Figure 1.1:** Occurrences mapping based on GPS data and speed estimation for overtaking maneuvers performed near cyclists. In this image two distinct scenarios are represented, a car performing an overtaking maneuver over 40 km/h and below 20 km/h, highlighted with red and green marks in the map, respectively.

## 1.1 Cyclists Numbers

In the last few years the number of cyclists has increased and this circumstance has given rise to the develop of systems to improve bicycle users' safety. Recent reports from Department for Transport from United Kingdom have revealed that in 2014 more than 20,000 cyclists were injured in reported road accidents. In Fig.1.2 the numbers regarding cyclist casualties are highlighted.

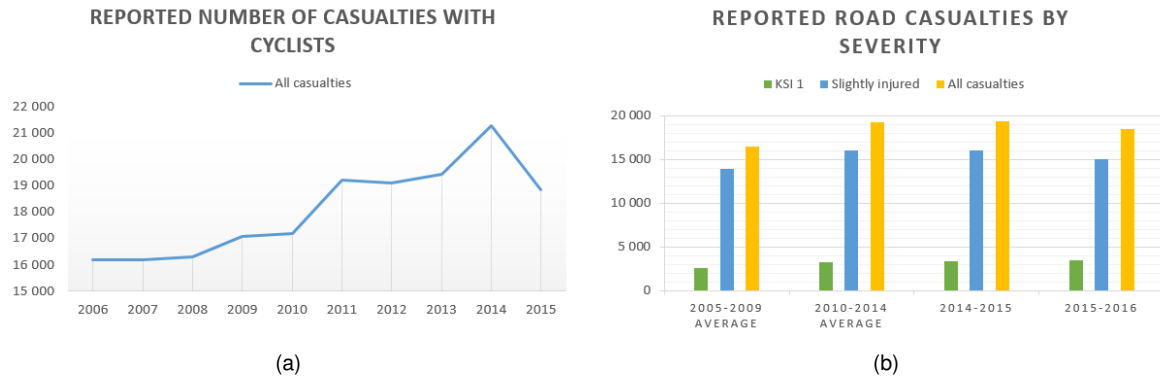


**Figure 1.2:** Reported road casualties (estimates) in UK, annual totals. Statistical release form the Department for Transport. (a) Number of casualties from 2006 to 2015; (b) Number of casualties by severity from 2006 to 2015.

Based on this report [11] from Department for Transport and analyses performed by The Royal Society for the Prevention of Accidents (RoSPA) [12] it is possible to emphasize the following statements:

- Most of the accidents take place in urban areas;
- Approximately two thirds of cyclists involved in accidents that lead to death or serious injuries were involved in collisions at, or near, a road junction;
- 80% of the accidents occur during daylight;
- Most of collisions involved a car.

Beside these general conclusions, it was also possible to pinpoint the most common cycling accidents, which may be taken into account for danger assessment. The casualties era presented as follows:

- Motor vehicle emerging into cyclist's path;
- Motor vehicle turning across cyclist's path;
- Cyclist riding into the path of a motor vehicle;
- Both vehicles moving straight ahead;
- Cyclist turning right from a major road and from a minor road;

Concerning Portugal, Autoridade Nacional Seguranca Rodoviaria (ANSR) [13] published reports on accidents from 2007 to 2016, which show an increase in number, as it is possible to conclude from Fig.1.3. However, this data is not representative due to the small sample of data regarding cyclists.

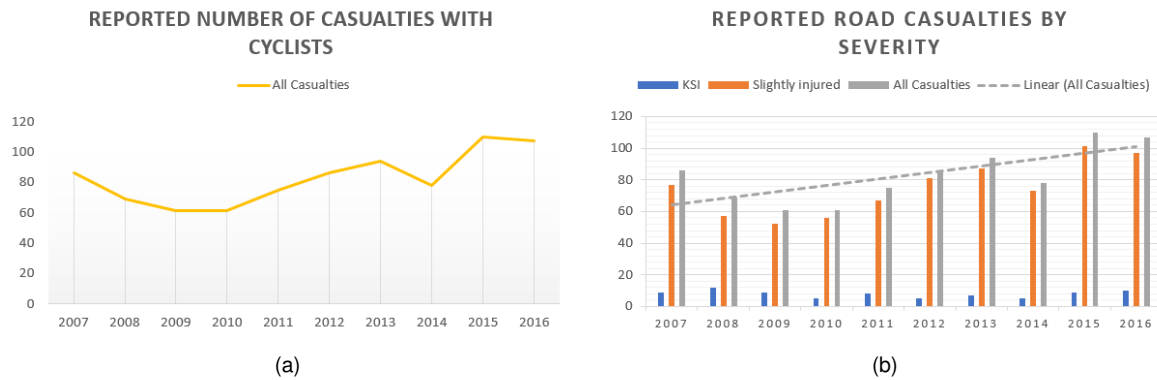


**Figure 1.3:** Reported road casualties (estimates) in Portugal, Statistical release from Autoridade Nacional Segurança Rodoviária. (a) Number of casualties from 2007 to 2016; (b) Number of casualties by severity from 2007 to 2016.

Since the reports on collision with cyclists in Portugal are too scarce to draw reliable conclusions from, the studies from the Department for Transport were used instead to find specific events that may be important to take into account and consider latter in future approaches.

Due to the lack of statistical data, classifying roads for cyclists with regard to safety has proved to be a major challenge. Even so, the numbers presented earlier in this chapter showed that the amount of bicycle's users have risen in recent years and that the amount of casualties have followed the same tendency. In this context, the need to create a system that may provide safer alternative paths in order to avoid dangerous situations from happening.

### 1.1.1 Mapping cyclists experience

In the last years, driving systems using smartphones as sensor platform have been developed. A list of the existing systems is presented bellow, as well as a brief description of its main features and goals.

- **Toronto Cycling App** [14]: Smartphone application that allows the users to gather data using a smartphone camera, together with GPS data, in order to performs an offline data examination that may be used for planning new transport facilities, namely cycle lanes.
- **Cyber-Physical bike** [15]: A system that aims to prevent dangerous situations and alerts the driver of proximity risks if a vehicle approaches from behind. A camera films the cyclist's rear and analyses how far the vehicle is from the cyclist and if this distance is less that a specified value the cyclist is alerted.
- **BikeCOM** [16]: Application prototype that relies on bicycle-to-vehicle communication to exchange safety relevant information and alerts the users to the presence of potential threats. With GPS data on position, speed and heading obtained through drivers' and cyclists' devices is possible to estimate the time-to-stop (TTS).

Other option is to diverge from accident prevention and instead focus on accident responsiveness. Such is the case of notification systems, tasked to immediately contact the emergency service in case an

accident happen. An example of this is eCall [17], a crash notification service for portable and nomadic devices, among others.

In our previous developments, in [2] and [1], event detection (overtaking, turning, stopping etc.), was performed based on the orientation of optical flow vectors in order to estimate direction and orientation of the surrounding objects [1]. Besides this, a new approach on how to identify maneuvers based on image processing techniques was presented concerning bicycles' environment.

With the same goal a proximity perception of the surrounding objects has been developed in [2]. This, together with the knowledge of cyclist trajectory based on the estimation of the focus of expansion, is used in order to predict potential collisions.

The proposed approach aims to add complementary information to the existing developed system, presented in Fig. 1.4, on the left side of the figure, the proposed module is highlighted. Combine previous systems results, [1] and [2], with this new module results will provide a more complete road characterization system.

Outside of bicycle specific studies, several approaches have been developed to analyze driving behavior. An important portion of them use multiple sensor systems to gather data, as in [18].

Others noteworthy studies follow different strategies, such as: detect risky driving patterns [19]; introduce a driver training system to prevent road accidents due to unsafe driving [20]; and provide driver assistance systems [21].

### 1.1.2 Data Acquisition

A smartphone application has been developed in previous works,[1] and [2], which allows to collect data from each cyclist's ride (Inertial Measurement Unit(IMU), video and audio). In this work, the following data acquired with the app will be used: date and time of the measurement; GPS coordinates (latitude and longitude); and speed from GPS (m/s).

The full scheme of all the features of the project are presented in Fig. 1.4. The *Cardio Stress Analysis* and *Road Surface Analysis* branches are here represented for completeness, but its usage is out of scope of this work.

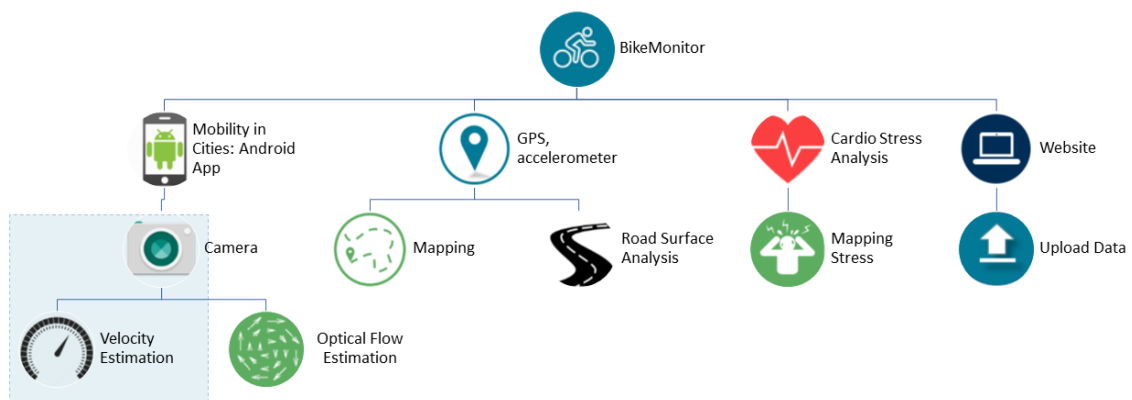


Figure 1.4: System Architecture

The resources available for video processing are very plain. The video images taken from either GoPro or smartphone camera, together with the use of the other sensors, are not enough to overcome low data quality due to unpredictable image variation, as a consequence of the erratic movement of the camera's support (bicycle handlebar).

## 1.2 General goals

The main goal of the presented work is the estimation of vehicles' speed in order to identify overtaking maneuvers performed in the cyclist's surroundings. Based on image processing and knowing the camera intrinsic parameters, a new approach to estimate vehicle proximity and speed is proposed based on license plate detection and tracking from data provided by a camera located at the bicycle's handlebar.

Several methods have been proposed to classify roads suitability regarding bicycles circulation, in [3] and [4], and lane width, vehicles speed and traffic flow are the most used parameters as well as events with vehicles are among the most risky situations [8]. As they are omnipresent indicators, the number of overtaking maneuvers and speed limit represent very important parameters in order to evaluate cyclist path's suitability.

## 1.3 Thesis Outline

The main goal of the presented work is the estimation of vehicle proximity and speed in order to identify dangerous maneuvers performed in cyclist's surroundings. A new approach to estimate vehicle proximity and speed is proposed based on license plate detection and tracking from data provided by a camera located at the bicycle's handlebar.

The document is organized in the following order. In the next chapter, an overall review concerning vehicles detection and tracking techniques is presented, in the context of driving systems. As well as a brief overview on license plate recognition techniques. In Chapter 3 the approach is explained in detail, being the most important steps presented as follows.

1. Vehicles detection and tracking based on license plate recognition.
2. Speed estimation.
3. Maneuver classification.

Experimental results are evaluated in Chapter 4, as well as speed error measurements. Final results allowed to geo-reference occurrences and perform an overall comparison between different roads. Finally, conclusions and future work are drawn in Chapter 5.

## Chapter 2

# Maneuver Identification System

### 2.1 State-of-the-Art

In recent years, several studies in the areas of Autonomous Driving have been developed, with special focus on vehicles detection, maneuvers evaluation and tracking. Playing a special role for traffic surveillance systems, they provide useful information for traffic flow control and evaluation.

Concerning vehicle detection and tracking, the use of a non-static camera represents a real challenge to estimate its pose and speed. Existing traffic surveillance systems are able to compute vehicles speed processing image from static camera records, based on motion vehicle detection techniques supplemented with lane and object detection techniques.

Streets classification systems concerning bicycles safety require complex systems and are still limited, once they require an investment in hardware to acquire information.

#### 2.1.1 Vehicle Detection and Tracking

Object detection represents a challenge in the field of image processing such as traffic flow control, automatic accident detectors and vehicles counting, among others. A lot of methods have been proposed, from background subtraction methods to more complex ones, based on motion estimation techniques.

Occluded vehicles, obstacles, or different lightning conditions are some of the challenges that could affect vehicles' detection.

Some advanced approaches of background subtraction methods, in [22] have been proposed in the last years combining statistical and parametric based techniques, with Gaussian probability distribution models, or feature detection for complex scenes, which has proven to improve its performance under poor illumination conditions and overcrowded scenes, as is presented in [23], in which a vehicle detection approach based on local features is proposed.

In [24] an adaptive background extraction algorithm based on Kalman filter and support vector machine (SVM) is proposed. In [25], an algorithm for vehicle recognition and tracking Gaussian mixture

models and blob detection model is presented, in order to count tracked objects for a traffic surveillance system.

To address the need of improving autonomous driving systems several benchmarks have been developed, such as KITTI [26] focus on object scene flow, estimating 3D motion fields, using two high resolution camera systems (grayscale and color), a laser scanner, and a localization system. A benchmark composed by mid-size-city environments, rural areas and highways with the aim of providing new challenges and difficulties to the computer vision community.

## 2.1.2 Vehicle Speed Estimation

In the field of driving systems, vehicle velocity estimation represents a topic of research and studies. In order to detect or predicted possible dangerous situations is necessary to compute a relative velocity of a vehicle that appears in the field of view.

Traffic surveillance systems have been developed in order to estimate vehicles' velocity, using stationary cameras. In [27], a Kalman filter based tracking system is applied in order to predict vehicles future location and velocity after an image segmentation process, which suffers a rectification process based on lane detection.

Similar approaches, as in [28] estimate vehicle speed considering a flat surface as a geometric constraint, background subtraction methods are applied for object detection, followed by Lucas-Kanade optical flow approach for tracking. Both apply projective transformations to original images in order to rectify them.

In [29], lighter computationally image processing techniques are applied to detect and track vehicles. A low-level license plate recognition is performed base on color information. Moving objects are detected based on background subtraction methods.

Tracking is performed based on the difference between vehicles' bounding box coordinates, and speed is estimated through a predefined imaginary lines cross space with known distances and size, if speed's values exceeds its limit, the extracted license plate is immediately transmitted to a remote station.

More recently, in [30] vehicle velocity estimation is performed with an average error of 1.12 m/s by resorting to deep learning architectures for depth and motion estimation and features extraction based on vehicle tracks, depth and motion.

In contrast to traffic surveillance systems that are under a fixed camera pose restriction, this approach observer is located on a moving platform, which increases problem's complexity due to the lack of information such as camera pose, ego-motion and foreground-background segmentation.

## 2.1.3 Events Detection

Several studies have been developed to analyze driving behavior. An important portion of them uses multiple sensor systems to gather data, as in [18]. Others noteworthy studies follow different strategies:

detect risky driving patterns [19]; introduce a driver training system to prevent road accidents due to unsafe driving [20]; and provide driver assistance systems [21].

In [17], a notification system immediately contact the emergency service in case of an accident occurrence, consisting of a crash notification service for portable and nomadic devices. Due to the seriousness of injuries caused in bicycle-car collisions and the need of immediately medical support, adapting these systems for cycling may offer benefits and better handle real life situations where emergency services must be contacted.

#### **2.1.4 Previous developments**

In previous developments of BikeMonitor, events estimation were performed based on the orientation of optical flow vectors in order to estimate the direction of the surrounding objects, [1]. A proximity perception of the surrounding objects has been developed in [2], together with the knowledge of cyclist trajectory based on the estimation of the focus of expansion, in order to evaluate potential collisions.

#### **2.1.5 License Plate Recognition**

Concerning traffic surveillance and security control systems, license plate recognition represents an important tool, making possible to identify traffic violation, tracking cars for urban surveillance systems, among others.

Due to environment variations, such as non-uniform illumination conditions, vehicle motion, viewpoint changes, and complex backgrounds scenes, license plate recognition has proven to be a real challenge.

Existing approaches work under restricted conditions, for instance stationary backgrounds or limited vehicle speed. Dynamic scenes with various working conditions, where plates appear with different sizes, orientations and positions combined with complex backgrounds increase the challenge's complexity.

Typically, license plate recognition involves two main stages: 1) license plate region detection and 2) license number recognition. Process all the pixels of an image, searching for specific characteristics is not feasible, since it would increase processing time, therefore some approaches based on specific features have been developed, focus on color, rectangular shape or texture in order to identify plates' region.

Since 1990, this topic has been a matter of study, from simple approaches based on color based methods, in [31] and [29], or edge based methods, as in [32] and [33], to more complex ones involving machine-learning methods.

Edge features methods are simpler and faster than more complex methods, however its performance highly depend on edges continuity.

Texture feature methods such as Haar-like features, which make the classifier invariant to brightness, color, size and position of license plates, or Gabor filters in [34], that allow to analyze texture in unlimited orientation and scales has proven to obtain good results, even in the presence of license plates' deformation, however these methods are computationally heavy.

Color feature methods are able to detect deformed plates with different inclination angles, however methods based on HSV color space are very sensitive to noise and RGB representation depends highly on illumination conditions.

An automatic recognition system is proposed, in [35], based on Convolutional Neural Networks (CNNs), trained over synthetic data, which recreates a wide range of illumination and perspective conditions.

In order to find a compromise between computational cost and results, some approaches combine more than one feature and different methods, such as in [24], in which a combination between Haar-like features and edge-based methods is proposed.

Recently, an open source Automatic License Plate Recognition library, OpenALPR [36], has been released. Detection module is performed with local binary patterns (LBP) algorithm, followed by possible license region identification and optical character recognition (OCR) techniques for character segmentation.

Also, regarding android application an automatic license plate recognition using a mobile device has been proposed in [37], license plate numbers are extracted in machine-encoded text type from images captured with devices' camera, applying two OCR methods [38], Tesseract engine and Neural Networks.

# Chapter 3

## Proposed Approach

The developed work is a vision-based vehicle detection and tracking system. It focuses on a vehicle's license plate, processing real-world data from cycling through the streets of Lisbon obtained with a camera located at the bicycle handlebar.

One of the main challenges of this problem has to do with the quality of the analysis data. This handicap is due both to the simplicity of available hardware (a non-static camera) and poor image quality, due to trepidation. This is a characteristic of bicycle trips not easily solvable, resulting in less stable and more noisy footage than of a vehicle's dash cam, for example.

The system has 4 main modules: 1) Vehicles Detection, 2) Vehicle Tracking, 3) Speed estimation, and finally 4) Maneuvers classification. In Fig. 3.1 the implementation process is presented.

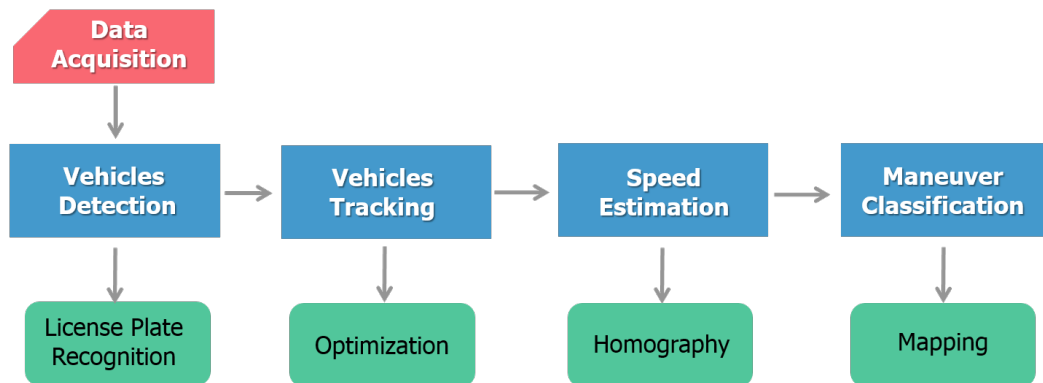


**Figure 3.1:** Implementation process from a vehicle's detection to maneuver identification.

All acquired data is uploaded through the app to the servers to be processed offline. During processing, each license plate vehicle is detected and tracked. An optimization problem is considered to match new detections with existing vehicles, and for each vehicle homography matrices are computed, between all detections of the same vehicle in sequences of images, in order to estimate speed. Based on speed values estimations is possible to identify overtaking maneuvers, and with GPS data provided by the app, map the occurrences.

Each module works independently from each other, for example the approach performed in the first stage for vehicle detection with license plate recognition could be replaced for any other detection

strategy, as long as the outputs maintain the same structure.

### 3.1 Data Set

The previous developed app [2] allows users to film their bicycle trips and upload them together with matching global positioning system (GPS) and inertial measurement unit (IMU) information to the server.

The data set includes road trips taken by different cyclists around Lisbon, in which the camera is located on the bicycle handlebar. In this work, GoPro acquired data was added to the existing data set for more street diversity. The following data acquired with the app will be used: date and time of measurements; GPS coordinates (latitude and longitude); and speed (m/s).

The resources available for video processing are very plain. The video images taken from either GoPro or smartphone camera, together with the use of the other sensors, are not enough to overcome low data quality due to unpredictable image variation, as a consequence of the erratic movement of the camera's support (bicycle handlebar) and trepidation.

### 3.2 Detection

Vehicles detection is performed using OpenALpr software in [36], which will provide both license plate corners coordinates and license plate character sequence. OpenALpr's image based process can be divided in two main steps: 1) Low level features analysis, in which a search of corners and edges is performed and 2) Character Analysis. The input elements correspond to an image or a video file. In Fig.3.2 the input and output image of this method are illustrated.

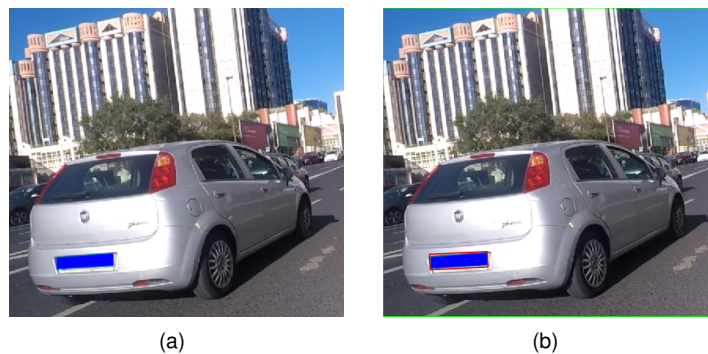


**Figure 3.2:** License Plate Recognition. (a) Input image; (b) Output image.

By inputting a frame of real-life footage, Fig. 3.2(a), OpenALpr outputs a license character combination and corresponding set of corner coordinates, Fig.3.2(b). These outputs will be used in the tracking module.

Each image is distorted, as shown in Fig. 3.3 taking into account a set of predefined homography parameters. This process improves detection accuracy and detect plates that could not be recognize due to the angles from where images were taken. This feature improves results for cameras filming at

close distance, from a fixed point and for scenarios where all plates that generally are seen at the same angle.

Once a specific maneuver is being analyze, it is possible to define an interval of values for orientation and position of plates and use this feature to identify plates of overtaking vehicles. An example is illustrated as follows.

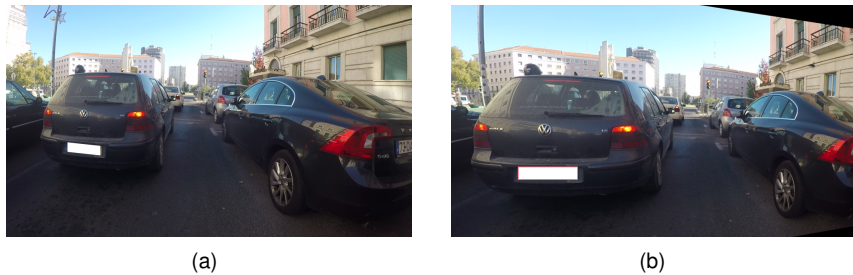


**Figure 3.3:** Homography distortion applied to an image. (a) Original image; (b) Distorted image.

OpenAlpr’s software is able to locate several license plates in a single image, and for each detection identify a subset of possible character combinations with corresponding confidence levels. In the first phase possible plate regions are identified with LBP algorithm [39].

After this, a character region identification is performed, if no possible regions are identified, the process begins for another image, otherwise another process begin. This first phase is responsible for identifying a possible region, that will be analyzed in the second phase in order to determine the most suitable edge, based on plate’s ideal dimensions and a list of possible horizontal and vertical lines (width and height), which are represented bellow, in Fig. 3.5.

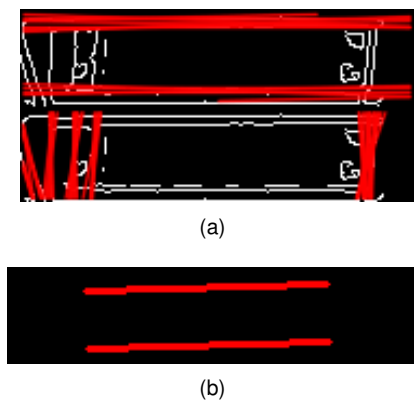


**Figure 3.4:** License Plate Region estimation. (a) Hough Lines; (b) Winning Lines.

The second phase is divided in four steps: 1) Plate edges identification, as explained above, 2) Deskew, 3) Character Segmentation and analyze and 4) Post processing.

After plate edges identification each image plate is remapped, removing distortion angles, and a character segmentation is performed based on vertical histogram analyses to find gaps between plate characters and discard edge regions that could lead to false identifications as well as dismiss regions with lack of information.

Each character is independently processed in OCR [38] stage, in which all possible characters and

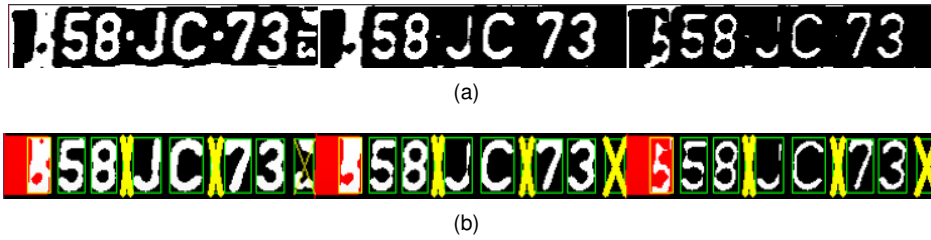


**Figure 3.5:** Character Segmentation. (a) Character Segmentation Input; (b) Character Segmentation Output.

correspondent confidences are determined.

Finally, possible plate character combinations are determined, all characters below certain thresholds are disqualified. Besides this, a region validation is possible taking into account license plate format to perform a match between results and plate format, allowing to discard results that do not correspond to the expected format. The final output correspond to a license character combination and corresponding set of coordinates, that will be used in the next step.

Through a configuration file, it is possible to define a set of homography parameters that could contribute to improve detection module performance, images suffer homography transformations based on these parameters.

In this context, define a good set of parameters that cover all the cases represented a major challenge. Therefore, 21 images with vehicles in different environments (lighting conditions, orientation, position, among other) were processed with different sets of configuration files. For each configuration file the number of successful detections were taken into account. The set of 3 configuration files able to successfully detect license plates on this specific data set were chosen as the final configuration set and applied in detection module.

Each video file was processed with 3 different configuration files, with this approach the number of detections increased in almost 1/3 of the number obtain if only one configuration file was used.

License's Plate sequence identification represents an advantage in order to detect and track specific vehicles. Therefore, its performance had to be taken into account in the tracking module. A brief analysis to letters sequence recognition have been performed, in which 335 detections were evaluated and results are presented in Table 3.1.

**Table 3.1:** License character sequence recognition performance.

Number of characters correctly identified	%
6	37.26
5	30.34
4	22.88
3	5.42
2	4.11

For instances, let's consider that a vehicle has been detected, in which the license plate sequence

is correctly identified in 8 frames. It is important to notice that these detections could have been taken in consecutive or spread moments of time. In 5 detections, only 4 letters have been correctly identified. Sequences with 4 and 3 characters have been identified in 5 and 3 frames, respectively. The tracking module must be prepared to deal with this small variations in order to considered a larger number of detections.

For this reason the cost variables defined in the tracking module, were determined taking into account not only license plate character sequence similarity as time and distance between detections contribution, in order to penalize the decision based not only on the number of similar letters, that may discard possible correct matches.

### 3.2.1 Outliers

One of the main challenges relied on discard possible outliers. Advertising in vehicles due to its characteristics lead to misleading detections, represented in Fig. 3.6. Identify outliers of specific events with few detections and evaluate them correctly represented a real challenge. For instances, the number of detections to parked cars vary from around 4 to 6 detections per vehicle, an error in one detection or more could lead to misleading results and influence events identification.



Figure 3.6: Other sequence of numbers is identified on the vehicles rare.

## 3.3 Vehicles Tracking

Based on licenses plate features and their location in the images it is possible to track vehicles in consecutive frames. The correspondence between detected plates in the current frame  $F$  and previous ones is computed solving the following linear program:

$$x^* = \operatorname{argmin}_x \quad c^T x \quad (3.1)$$

$$\text{s. t.} \quad Ax \leq b \quad (3.2)$$

$$A_{eq}x = b_{eq} \quad (3.3)$$

$$x \geq 0 \quad (3.4)$$

where  $x$  is the stacked vector of matrix  $X$ , presented in (3.5) and represents the optimization variable, and  $c$  is the stacked vector of matrix  $C$ . Considering  $m$  vehicles in frame  $F - 1$  and  $n$  detections in frame  $F$ , matrix  $C$  and  $X$  are given by

$$X = \begin{bmatrix} x_{11} & x_{12} & \cdots & x_{1m} \\ x_{21} & x_{22} & \cdots & x_{2m} \\ \vdots & \vdots & \vdots & \vdots \\ x_{n1} & x_{n2} & \cdots & x_{nm} \\ x_{n+1,1} & x_{n+1,2} & \cdots & x_{n+1,m} \end{bmatrix} \quad (3.5)$$

$$C = \begin{bmatrix} c_{11} & c_{12} & \cdots & c_{1m} \\ c_{21} & c_{22} & \cdots & c_{2m} \\ \vdots & \vdots & \vdots & \vdots \\ c_{n1} & c_{n2} & \cdots & c_{nm} \\ c_{n+1,1} & c_{n+1,2} & \cdots & c_{n+1,m} \end{bmatrix} \quad (3.6)$$

Each element,  $c_{nm}$ , represents the final cost of associating a new detection,  $n$ , with the previous vehicle,  $m$ . For instance, if  $x_{nm}$  is equal to the value one then the cost,  $c_{nm}$ , of associating a new detection,  $n$ , with a previous vehicle,  $m$ , will be selected. Since matrices  $A$  (3.2) and  $A_{eq}$  (3.3) are totally unimodular, the solution of this convex optimization problem is integer [40].

In order to improve method robustness concerning possible errors of license plate detection (e.g. characters and location misleading), the last detections of a vehicle  $m$  occurred at frames  $F$ ,  $F - 1$  and  $F - 2$  were considered as the following expression shows,

$$c_{nm} = wb_1 c_{nmF} + wb_2 c_{nmF-1} + wb_3 c_{nmF-2} \quad (3.7)$$

The cost of associating a new element  $n$  to a specific detection of a vehicle  $m$  in a certain frame  $F$  is given by  $c_{nmF}$ , which depends on the number of similar letters, distance between license's centroids in consecutive frames and lapsed time.

$$c_{nmF} = l_{nmF} - w_1 \log\left(\frac{\delta_d}{d_{nmF}}\right) - w_2 \log\left(\frac{\delta_r}{r_n - r_v}\right) \quad (3.8)$$

The term  $l_{nmF}$  quantifies how many similar letters a new license plate  $n$  and a tracked license plate  $m_F$  have in common. Since character recognition output results for the same license plates varies in different instance, there was the need to add more variables, taking into account the difference between centroids and time intervals.

The term  $d_{nmF}$  expresses the difference between centroids of licenses  $m_F$  and a new detection  $n$ . Here, logarithm function is used in order to penalize the part of the cost function associated with  $l_{nmF}$  values. For values above the defined threshold  $\delta_d$ , the cost value increases. Otherwise, when the distance between the centroids is small, the cost function decreases, which contributes for a possible matching.

A time contribution part has to be taken into account, once an overtaking maneuver is performed at short instances of time. Time intervals above a certain threshold  $\delta_r$  penalize the final cost value  $c_{nm_F}$ . The variables  $r_n$  and  $r_v$ , represent current time instance and the last time vehicle  $m$  was detected, respectively. The influence of time and distance between licenses centroids is determined by a set of *weights*  $= [w_1, w_2]$ , which were tuned empirically.

Finally, the set that includes all active tracked vehicles is given by  $\mathcal{V} = \{v_1, v_2, \dots, v_m\}$ , which includes for each vehicle a subset of  $m_F$  detections of the same vehicle. If there is no possible correspondence between a new detection  $n$  and tracked vehicles in  $\mathcal{V}$ , a new vehicle is added to  $\mathcal{V}$  and in the next iteration a new column will be added to the cost matrix. In order to deal with new detections without correspondences, we add an extra row to  $C$  in Equation (3.6) where each entry -  $c_{n+1,1}, \dots, c_{n+1,m}$  - has the same value  $\gamma$ .

In this stage, all tracked vehicles in the subset  $\mathcal{V}$  are obtained by solving the optimization problem (3.1-3.4) for each frame.

A simple problem instance is represented in 3.9, in order to illustrate these concepts, where matrix  $\mathcal{C}$  represents the cost matrix and  $c_{nm}$  correspond to the cost of associating a new detection  $n$  to a previous vehicle  $m$ . The number of columns of  $\mathcal{C}$  represents the number of previous detected vehicles ( $\max\{m\} = 4$ ), with which the new detection must be compared.

$$C = \begin{bmatrix} c_{11} & c_{12} & c_{13} & c_{14} \\ \gamma & \gamma & \gamma & \gamma \end{bmatrix} \quad (3.9)$$

In this example when a new detection  $n$  is processed, there are 4 vehicles on the tracking set  $\mathcal{V}$  that can be a possible match with the new vehicle. Here, each entry -  $c_{n+1,1}, \dots, c_{n+1,m}$  - has been substitute with the value  $\gamma$ . If no match is found, i.e.  $c_{1m} > \gamma$ , for each value of  $m = \{1, 2, 3, 4\}$ .

When more than one license plate is identified per frame, for instances  $n = \{1, 2\}$ , a new line is added to the Cost Matrix, represented in 3.10.

$$C = \begin{bmatrix} c_{11} & c_{12} & c_{13} & c_{14} \\ c_{21} & c_{22} & c_{23} & c_{24} \\ \gamma & \gamma & \gamma & \gamma \end{bmatrix} \quad (3.10)$$

If there is no possible correspondence between a new detection  $n$  and tracked vehicles in  $\mathcal{V}$ , a new vehicle is added to  $\mathcal{V}$  and in the next iteration a new column will be added to the cost matrix. In the other hand, if a match is found, the new element  $n$  will be introduced on the subset  $m_F$  of the corresponding vehicle in the set  $\mathcal{V}$ .

This stage is completed when all the elements of detection output are analyzed. The final output is a matrix with all tracked vehicles  $\mathcal{V}$ , in which for each element  $v_m$  a subset  $m_F$  with license sequence, corners coordinates and time instance information is associated.

Since overtaking maneuvers occur in small instances of time, i.e. between several detections of the same vehicle performing an overtaking maneuver the time difference between consecutive detections correspond to 3-5 frames (0.12-0.4 seconds). There is no advantage of comparing new detections with

old detected vehicles, therefore a set of active vehicles in  $\mathcal{V}$  is taken into account to compare with a new detection  $n$ . In other words, a current detection  $n$  is compared with all previous detected vehicles inside a time window, as illustrated in Fig.3.7.

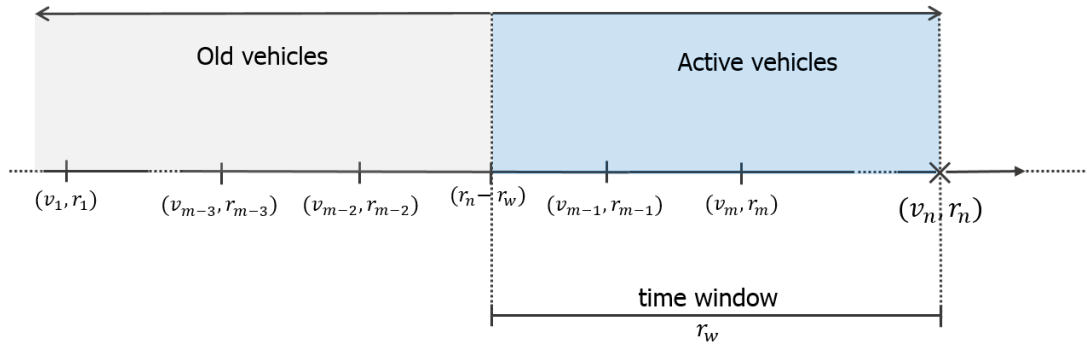


**Figure 3.7:** Scheme representing the subset of active vehicles to compare with a new detection  $n$ , defined by a time window  $[r_n - r_w, r_n]$ .

In summary, for each new detection  $n$  only a subset  $\mathcal{V}'$ , with the most recent tracked vehicles, will be considered. It is worthy to note that even if this time window was not applied these old detections would be discarded in Equation (3.8), since a time parcel is taken into account. The value of the cost  $c_{nm}$  will increase to infinite for old detections, that would be automatically discard as possible matches.

Once tracking module has finished, a matrix with all detections for each vehicle is generated. Each element of tracked vehicles contains information concerning time instance and license plate coordinates.

### 3.4 Vehicle Speed Estimation

In order to estimate the transformation and rotation of a planar object in two images it is necessary to compute and decompose the homography matrix, which allows to map an object in the first image into the second image and vice-versa. In image processing field, this is a common technique to estimate pose, compute 3D objects' reconstruction with several 2D images and perspective correction, among others.

The camera displacement can be extracted through an homography decomposition process. The relationship between two corresponding points  $q (q^x, q^y)$  and  $q' (u, v)$  can be described as:

$$\lambda \begin{bmatrix} q^x \\ q^y \\ 1 \end{bmatrix} = H \begin{bmatrix} u \\ v \\ 1 \end{bmatrix} \quad (3.11)$$

where  $\lambda$  represents a scalar factor and  $H$  is a  $3 \times 3$  homography matrix, given by  $H = \begin{bmatrix} h_{11} & h_{12} & h_{13} \\ h_{21} & h_{22} & h_{23} \\ h_{31} & h_{32} & h_{33} \end{bmatrix}$ .

Solving equation (3.11), it is possible to obtain the following equations:

$$-h_{11}q^x - h_{12}q^y - h_{13} + (h_{31}q^x + h_{32}q^y + h_{33})u = 0 \quad (3.12)$$

$$-h_{21}q^x - h_{22}q^y - h_{23} + (h_{31}q^x + h_{32}q^y + h_{33})v = 0 \quad (3.13)$$

These equations can be represented in a matrix form

$$A_i h = 0 \quad (3.14)$$

where  $A_i$  is a  $2 \times 9$  matrix, and  $h$  is a vector with 9 elements with the entries of matrix  $H$ .

$$A_i = \begin{bmatrix} -q^x & -q^y & -1 & 0 & 0 & 0 & uq^x & uq^y & u \\ 0 & 0 & 0 & -q^x & -q^y & -1 & vq^x & vq^y & v \end{bmatrix}, \quad (3.15)$$

$$h = [h_{11} \ h_{12} \ h_{13} \ h_{21} \ h_{22} \ h_{23} \ h_{31} \ h_{32} \ h_{33}]^T, h_{33} = 1$$

Each point correspondence provides two independent equations. Since  $H$  has 8 degrees of freedom, given a set of four corresponding points, it is possible to find a solution. From this set of points we can define a set of equations  $Ah = 0$ , in which  $A$  is formed by the elements of each matrix  $A_i$ , for each corresponding points, and  $h$  is the vector of unknown entries of matrix  $H$ . Final  $A$  matrix will have dimension  $8 \times 9$  and a 1-dimensional null-space that corresponds to the solution space for  $h$ .

## Pose Estimation

Considering  $P_i$  as the reference plate coordinates in the 3D world and  $p_i$  the points on the image of the reference frame, it is possible to write the following map

$$\begin{bmatrix} u'_i \\ v'_i \\ \lambda_i \end{bmatrix} = K \begin{bmatrix} R & t \end{bmatrix} \cdot \begin{bmatrix} p_i^x \\ p_i^y \\ p_i^z \\ 1 \end{bmatrix}, i \in \{1, 2, 3, 4\} \quad (3.16)$$

where  $K$  is the intrinsic camera matrix,  $R$  a rotation matrix,  $t$  a translation vector and  $\alpha$  a scalar factor. Regarding to the reference plate,  $P^i = [p_i^x \ p_i^y \ p_i^z]$  is the 3D location of corner  $i$ . Since the camera observes a planar object, it is possible to consider the reference plate at the plane  $p^z = 0$  and estimate the homography matrix, presented as follows.

$$\lambda_i \begin{bmatrix} u_i \\ v_i \\ 1 \end{bmatrix} = K \underbrace{\begin{bmatrix} R' & t \end{bmatrix}}_H \cdot \begin{bmatrix} p_i^x \\ p_i^y \\ 1 \end{bmatrix} \quad (3.17)$$

where the pair  $(u_i, v_i)$  represent the 2D projection of corner  $i$  and  $R'$  contains the two first columns of  $R$ .

With à priori knowledge of license plate dimensions ( $p_i^x$  and  $p_i^y$  are known), together with the detection

of license's 4 corners in the image it is possible to compute homography matrix  $H$ , defining for each license plate corner the values  $A_i$  of Equation (3.15), consequently determine the set of equation  $Ah = 0$  for all points and compute the solution space for  $h$ .

Since it is possible to compute  $H$  and the intrinsic camera matrix  $K$  is known,  $R'$  matrix and translation vector  $t$  are estimated according to

$$\underbrace{K^{-1}H}_G = \alpha \begin{bmatrix} R' & t \end{bmatrix} \quad (3.18)$$

Given matrix  $G'$  composed by the first two columns of  $G$ ,  $R'$  is the closest orthogonal matrix closest to  $G'$  as the following optimization problem states

$$R' = \operatorname{argmin}_X \quad \|G' - X\|_F^2 \quad (3.19)$$

$$\text{s. t.} \quad X^T X = I \quad (3.20)$$

Although this problem is non-convex due to the constraint, it has a closed-form solution. Computing the singular value decomposition (SVD) of  $G'$ ,

$$G' = U \begin{bmatrix} \lambda_1 & 0 \\ 0 & \lambda_2 \end{bmatrix} V^*, \quad (3.21)$$

$R'$  is given by

$$R' = UV^*, \quad (3.22)$$

Estimating  $R'$ , the translation vector  $t$  and the scalar factor  $\alpha$  are computed according to the following expressions

$$\alpha = \frac{\lambda_1 + \lambda_2}{2}, \quad (3.23)$$

$$t = \frac{G''}{\alpha} \quad (3.24)$$

where  $G''$  is the last column of  $G$ .

For each vehicle, rotation  $R^m = \{R_{(c_1, l_1)}^m, R_{(c_2, l_2)}^m, \dots, R_{(c_F, l_F)}^m\}$  matrices and translation  $t^m = \{t_{(c_1, l_1)}^m, t_{(c_2, l_2)}^m\}, \dots, t_{(c_F, l_F)}^m)$  vectors are computed between several license plates for the same vehicle  $m$ . Considering that each  $R^m$  and  $t^m$  correspond to the transformation applied to the camera coordinates in order to see all license plate in  $p^z=0$ , i.e. the camera moves in relation to the reference plate ( $l_1^m = l_2^m = \dots = l_F^m$ ). This approach is described in Fig. 3.8.

Notice that  $t_{c_{ij}}$  is equivalent to  $t_{ij}$  once the translation between camera coordinates  $c_i$  and  $c_j$  will be the same as between license coordinates  $l_i$  and  $l_j$ , therefore from now on the most simplified notation will be used, where  $i$  and  $j$  represent two license plates of the same vehicle detected in different time instances.

The translation vector between license plates in two different frames  $(i, j)$  can be computed as  $t_{(i, j)}^m = t_j^m - t_i^m$ . In  $F$  frames, we have the set of translation vectors between consecutive license plates of a vehicle  $m$  given by,  $t^m = t_{(1, 2)}^m, \dots, t_{(1, F)}^m, \dots, t_{(F-1, F)}^m$ .

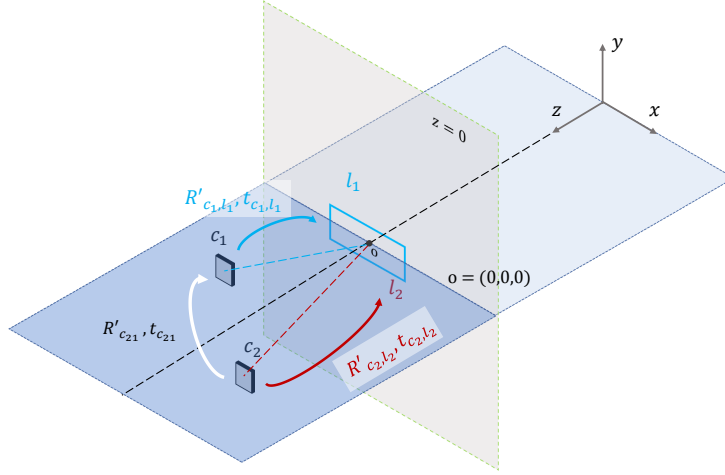


**Figure 3.8:** Rotation matrices and translation vectors estimation between two detections.

This being said, it is possible to compute translation vectors between all camera coordinates,  $t^m = \{t_{c_{12}}^m, t_{c_{13}}^m, \dots, t_{c_{bF}}^m\}$ , where  $b$  represents the number of possible combinations of  $m_F$  elements taken 2 at a time,  $b = \frac{m_F!}{(m_F-2)!2!}$ .

In this case, we can compute the speed for each translation vector, based on the translation values  $t_{(i,j)}^m$  and corresponding time intervals. A new set  $sp^m = \{sp_{(1,2)}^m, \dots, sp_{(1,F)}^m, \dots, sp_{(F-1,F)}^m\}$  is defined, where  $sp_{(i,j)}^m = \|t_{(i,j)}^m\| / (r_j - r_i)$  and  $\Delta dist_{(i,j)} = \|t_{(i,j)}^m\|$ . This values, together with corresponding time intervals allow to compute speed final values  $sp = \{sp_1, sp_2, \dots, sp_b\}$ , given by

$$sp_i^m = \frac{\Delta dist_{(i,j)}^m}{r_i - r_j} \quad (3.25)$$

where variables  $r_i$  and  $r_j$ , represent detection's time instance, and  $\Delta dist_{(i,j)}$  represents the distance between the coordinates of camera  $c_i$  and  $c_j$ . Distance estimation between two license plates detected at different time instances is represented in Fig.3.9. For simplicity reasons, in the example presented the camera moves only along z-axis (no variation along x-axis and y-axis), and as a consequence  $\Delta dist_{(i,j)}^m = \Delta z_{(i,j)}^m$ .

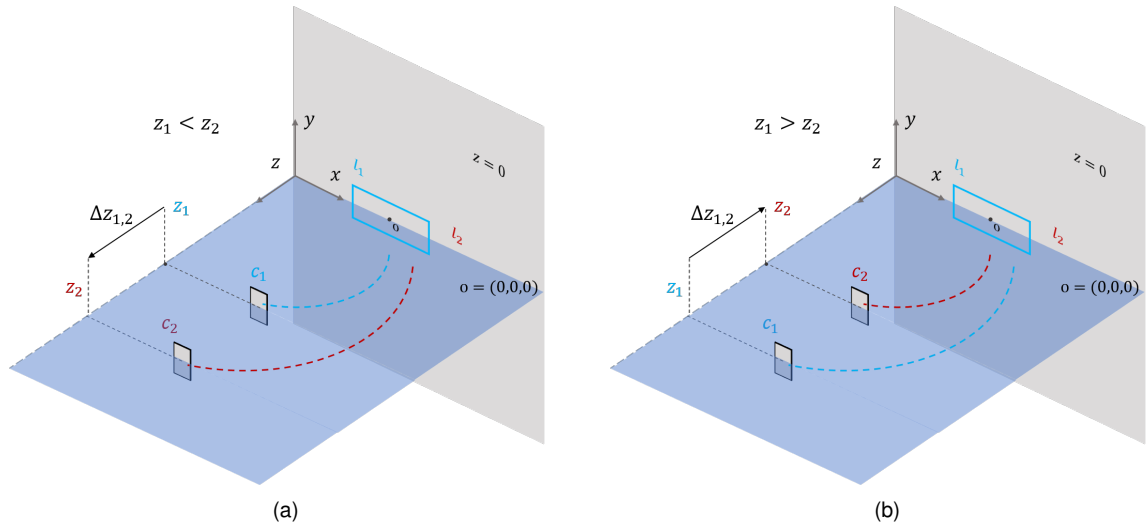


**Figure 3.9:** Distance measurement between two detections,  $l_1$  and  $l_2$  represent two license plates detected at different instances of time. (a) Vehicle performing an overtaking maneuver,  $z_2 > z_1$ ; (b) Cyclist performing an overtaking maneuver,  $z_2 < z_1$ .

### 3.5 Maneuver Identification

This being said, it is possible to distinguish if the camera is approaching or moving away, which is equal to determine if the vehicles (license plates) are moving away or approaching respectively and consequently determine if the cyclist is being overtaken by a vehicle or if it is performing an overtaking maneuver to a vehicle, as it is illustrated in Fig. A.1.

An overtaking maneuver is illustrated in Fig. 3.10, in which a vehicle is detected and tracked for 0.6 seconds, 15 successful detections were performed, and the final value of speed computed (31.49 km/h.) Based on Fig.3.11, it is possible to conclude that the vehicle travels approximately 3 meters and

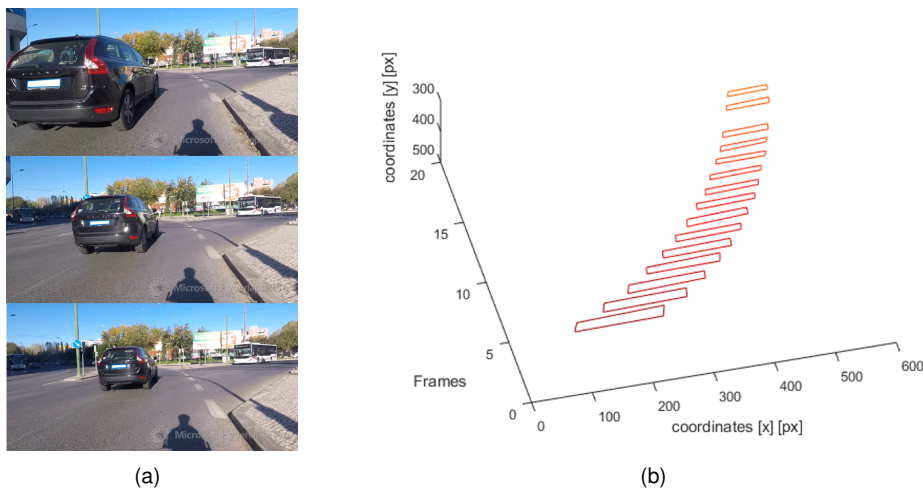


**Figure 3.10:** Overtaking maneuver example. (a) Vehicle detected performing an overtaking maneuver; (b) 2D Representation of all detections of the same vehicle with respect to time.

that the measurements become irregular with distance, which is expected since detection performance decreases with distance. A different perspective is presented in Fig. A.2, in which it is possible to

observe that the vehicle moves not only on the z-axis (straight line) but also on the x-axis, describing the expected behavior of an overtaking maneuver performed at a left turn.

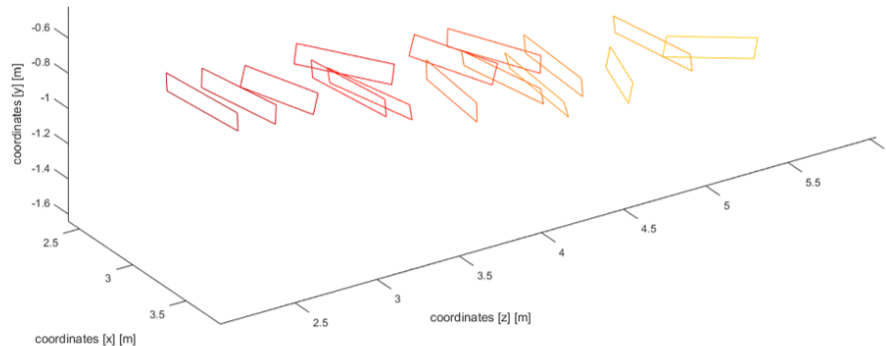


**Figure 3.11:** 3D Representation of all detections of a vehicle performing an overtaking maneuver.

In the other hand, when a cyclist overtakes a vehicle (parked or moving) the values along the z-axis decrease. An example of an overtaking maneuver performed by a cyclist to a parked vehicle is presented in Fig. 3.12. Once the vehicle is approaching vehicles speed is expected to be negative in the bicycle reference frame, and null in the world reference plan.

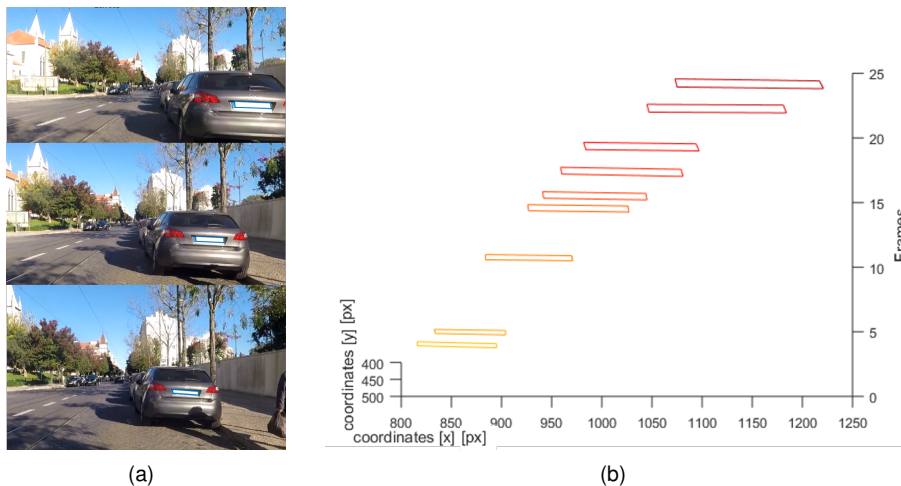


**Figure 3.12:** Cyclist overtakes parked vehicle. (a) Vehicle parked at the right side of the road; (b) 2D Representation of all detections of a parked vehicle with respect to time.

In this case cyclist is slowly approaching the vehicle, 9 detections were performed, which allowed to estimate vehicle speed ( $\approx$ -16 km/h) with respect to the bicycle reference frame and conclude that an overtaking maneuver is performed by the cyclist. A 3D reconstruction of the scene is presented in Fig. 3.13, the values along the z-axis decrease as the cyclist approaches the vehicle. In Fig.A.3 a different perspective is presented.

Theoretically, it would be possible to define a set of four line that intersect the cornes of each license plate on the 3D image, however due to detection errors this is not possible and the error will influence 3D

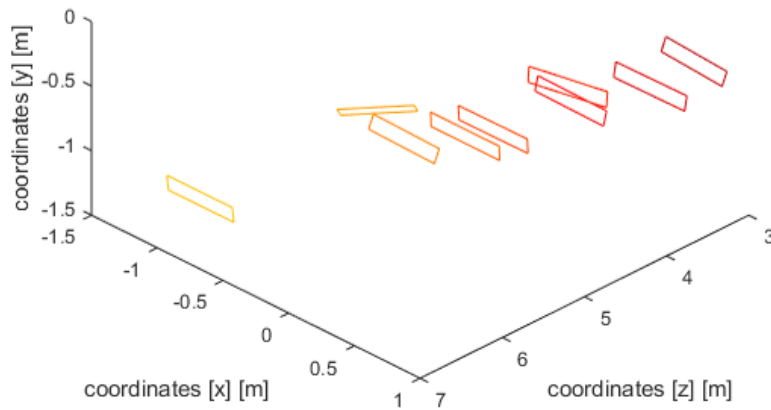


**Figure 3.13:** 3D Representation of all detections of a parked vehicle.

reconstruction results. Small variations of detected points on the 2D image represented in Fig. 3.10(b) could lead to misleading results on the 3D reconstruction in Fig. 3.11. In Fig. 3.12(b), from the 6th to the 7th detection license plate area incorrectly decreases, which will affect the 3D reconstruction and lead to misleading results, as it is represented in Fig.3.13 and in Fig.A.3 , the reconstruction of detection number 7 is incorrect.

### 3.6 Mapping

Detection and tracking results together with GPS data gathered with a smartphone, allowed to identify where the overtaking maneuvers occurred, and characterize specific streets and neighborhoods. For each trip, an occurrences map has been created, in Fig. 3.14 an example is presented. A color range was defined in order to represent certain speed intervals, presented as follows.

**Table 3.2:** Color range representation for speed intervals

Speed	Color
$sp \leq 20$	green
$20 < sp \leq 30$	yellow
$30 < sp \leq 40$	orange
$40 < sp \leq 50$	red
$sp > 50$	black



**Figure 3.14:** Georeference of overtaking maneuvers detected for a single trip.



# Chapter 4

## Results

### 4.1 Overtaking Maneuver Identification

More than 7 hours of bicycle trips were processed, with almost 120 kilometers traveled at different times of the day. Results analysis allowed to conclude that detection performance decreased with distance. Therefore, 3 types of overtaking maneuvers were considered in order to perform a detailed evaluation based on lane delimitation. Identifying overtaking maneuvers performed near cyclists is extremely important in order to assess the potential danger and characterize roads concerning bicycles suitability. Results analysis concerning each type of maneuver are presented in Table 4.1.

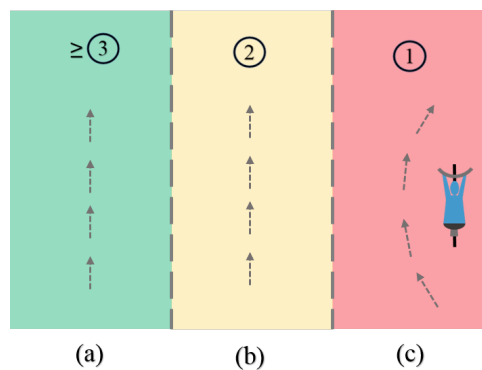


**Figure 4.1:** Overtaking zones based on lane division. (a) Overtaking type 3; (b) Overtaking type 2; (c) Overtaking type 1.

A scheme of the predefined zones is illustrated in Fig. 4.1, which aims to represent several possible scenarios, in which the tests have been performed, such as roads inside neighborhoods with only one lane to share to more complex environments (increased traffic flow, number of lanes, parking areas, among others).

Determine detection's performance for overtaking maneuvers of type 1 and estimate vehicles' speed error will be the main focus of this evaluation. Each time a vehicle overtakes a cyclist sharing the same lane it is considered as an overtaking of type 1. Overtaking maneuvers performed for more than three lanes apart from the cyclist were considered as type 3, in Fig. 4.1(a), and will not be considered for

results analysis, once it is not possible to identify license plates above 2 lanes apart from the cyclist.

**Table 4.1:** Detection results for each type of overtaking maneuver.

Overtaking Maneuver	Detected	(%)	Total
Type 1	187	78.9	237
Type 2	143	47.9	298

A total of 187 overtaking maneuvers of type 1 over 237 were correctly identified. False positives (FP) correspond to misleading results due to incorrect detection or tracking of vehicles. Tracking of parked vehicles and advertising areas correspond to 5.71 % of the total number of identified maneuvers.

All overtaking maneuvers of type 1 that failed to be identified have been considered as false negatives (FN), 21.1%. However, it is worthy to differentiate possible maneuvers that failed to be identified in Fig. 4.2(b) from others that are not possible to identify due to poor image quality or lightning conditions, in Fig.4.2(a). Considering this, 2 types of false negatives have been defined. For 50 missed detections, 74% of overtaking maneuvers were considered to be failed and 26% could not be identified. In summary, from the total number of detections, 15.61% were not correctly identified, in which 5.49% were not possible to identify with this approach.



(a)



(b)

**Figure 4.2:** False negatives representation. (a) Overtaking maneuver missed due to trepidation, it is not possible to identify a license plate.; (b) Overtaking maneuver missed, lightning conditions and reflections influence detection performance.

Since the performance of this approach depends strongly on detection performance, which decreases with distance, failed detections of overtaking maneuvers performed at more than 2 lanes apart from the cyclist were not considered for this evaluation.

Poor lightning conditions and poor image quality due to the natural trepidation caused by bicycle movement, makes this detection a real challenge once license plate identification depends heavily on lightning condition and image stabilization. Speed estimation is based on the coordinates of detected license plates, which if not correctly estimated could lead to incorrect speed estimation measurements.

Analyzing the results presented in Table 4.1 it is possible to take the following conclusions concerning overtaking of type 1:

- **78.9%** of overtaking maneuvers were correctly identified.
- **5.71%** of the detections performed are false positives.

Regarding, overtaking maneuvers of type 2, only 47.9% were identified, which emphasizes how overtaking maneuver detection performance decreases with distance.

## 4.2 Speed Estimation Error

As far as the authors are aware, there is no available data set with ground truth values concerning vehicle's speed estimation moving at bicycles surrounding, and with image sequences taken on a bicycle.

This being said, in order to compute speed estimation error, 95 overtaking maneuvers were analyzed. The real license plate coordinates were determined by hand and the correspondent speed values computed. Final results were determined for two distinct events: 1) vehicle overtakes bicycle and, 2) bicycle overtakes vehicle, with 4.5 km/h and 6.34 km/h of error, respectively.

The significant difference between the error of being overtaken and be the one that overtakes, is due to the fact that mostly of the overtaken vehicles associated with a large error correspond to parked cars. In this cases, the cars emerge at the right side of the road and a small number of detections is performed for each vehicle. Few detections to a vehicle hinder outliers identification performed in the tracking module.

The parameters defined in vehicle detection module, were chosen to identify licenses for overtaking maneuvers performed at bicycle's left side, in detriment to the right side. Therefore an increased error for vehicles merging at bicycles' right side is expected.

## 4.3 Application

The traveled areas were segmented into 7 zones, as shown in Fig.4.3. For each area a subset of roads were selected to perform a detailed comparison and possible conclusions. A brief description of each area is presented as follows.

- Area A: represents a small neighborhood (Campo de Ourique) with roads with only one lane and parking areas.
- Area B: roads with more than 2 lanes, where the average speed and traffic flow increase.
- Areas C: roads with one to two lanes, cycle lanes and mixed traffic zones (speed limit above 30 km/h).
- Area D: roads with one to three lanes and large roundabouts.
- Area E: roads with one to two lanes, cycle lanes and large roundabouts.
- Area F: main avenue that connects to the historical center.

- Area G: historical center, requested area that is under restricted circulation laws, due to the overload vehicles circulation. Cycle lane areas.

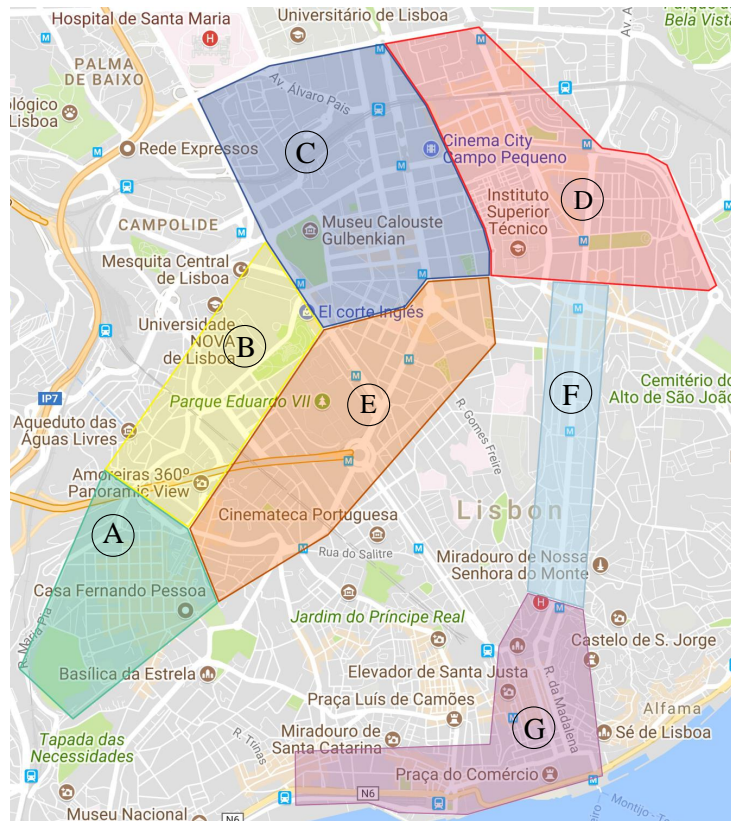


**Figure 4.3:** Representation of traveled areas segmented into 7 different zones.

A total of 288 overtaking maneuvers have been identified in these areas, final results are presented in table 4.2. Based on the results obtained it was possible to draw the following conclusions.

More than 70% of overtaking maneuvers that occurred inside neighborhoods are performed below 30 km/h. This values are highlighted in Table 4.2 for areas A and C. In the other hand, areas with roads with increased number of lanes and traffic flow, as in area B present more than 60% of overtaking maneuvers performed above 30 km/h.

In area D, results seem to be distributed in all ranges, this suggests that this area could be divided into two different area in order to obtain more conclusive results. In area E, 75% of overtaking maneuvers were detected at less than 30 km/h. Similar to area A, area G is by far the area where overtaking maneuvers were performed with the lowest speed, 85.71% of overtaking maneuvers were performed under 30km/h, fact that could be explained by the existence of several cycle lanes on this area.

Finally, area F represents a main street, that connects to the historical center of the city, and as a consequence is the street with less video samples and more overtaking maneuvers detection (28%) over the total number of overtaking maneuver detections for the entire data set, which emphasizes how requested this street is compared with others. In this street, 60% of the overtaking maneuvers were performed above 30 km/h. In this particular street, represented in Fig. 4.7(b) it is worthy to notice that vehicles speed decrease close to the intersections, at the beginning and the end of the path highlighted

in Fig.4.7(a).

**Table 4.2:** Overtaking maneuvers detections results with area and speed range specification.

Speed <sub>(sp)</sub> [km/h] \ Area	A	B	C	D	E	F	G	Total
sp ≤ 20	59.09%	12.20%	50%	22.41 %	27.78%	24.36 %	66.67%	84
20 < sp ≤ 30	18.18%	21.95%	18.75%	15.52%	47.22%	15.38%	19.05%	61
30 < sp ≤ 40	13.64%	43.90%	18.75%	25.86%	19.44 %	24.36%	9.52%	69
sp > 40	9.09%	21.95%	12.50%	36.21%	5.56%	35.90%	4.76%	66
Total	22	41	32	58	36	78	21	288

### 4.3.1 Characterization

For each area, a set of main roads were chosen for evaluation purposes. These roads are possible candidates to suffer changes in order to increase the network of bike lanes [41]. In Table 4.3, for each road the main characteristics are highlighted.

#### Area A: Campo de Ourique

In this residencial area with streets with only one lane and parking areas 77% of detected maneuvers were performed under 30 km/h, with 59% above 20 km/h. Besides this, compared with the results of other areas presented in Table.4.2, only 7.6% of the total number of detected overtaking maneuvers occurred in this area. This can be explained by the fact that in this area each street has only one lane and parking areas in both sides of the road which may hamper drivers to perform overtaking maneuvers.

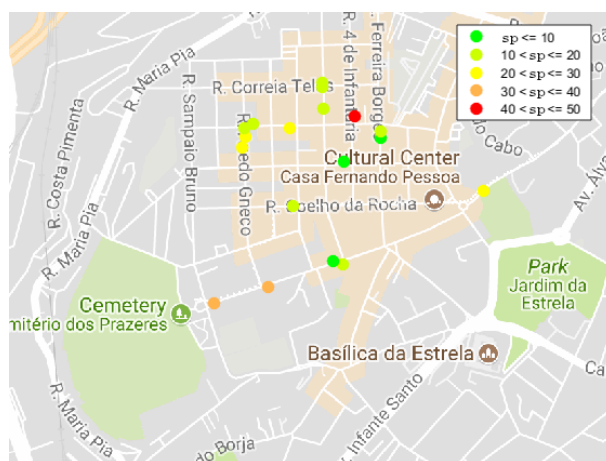


**Figure 4.4:** Representation of all overtaking maneuvers detected in Campo de Ourique.

#### Area B: Avenida Conselheiro Fernando de Sousa and Rua Carlos Alberto da Mota Pinto

In this area represented in Fig. 4.5(a) the traffic flow increases ( 14%) comparatively to area A (7.6%), once the streets covered in this area, present completely different characteristics. Avenida Conselheiro

Fernando de Sousa highlighted in Fig.4.5(a) has 3 lanes for each direction, parking areas on the right side of the road and ends at a complex intersection. The results reflect these characteristics with 93% of overtaking maneuvers performed above 30 km/h.

After the intersection Rua Carlos Alberto da Mota Pinto emerges with only 2 lanes, connected with Avenida Conselheiro Fernano de Sousa through a complex intersection. The number of detected overtaking maneuvers has remain the same for the two streets, however a difference between the values for speed is noticed. In Rua Carlos Alberto da Mota Pinto 43% of overtaking maneuvers were detected below 30 km/h, in contrast to Avenida Conselheiro Fernano de Sousa, in which 40% of the overtaking maneuvers were detected above 40 km/h.

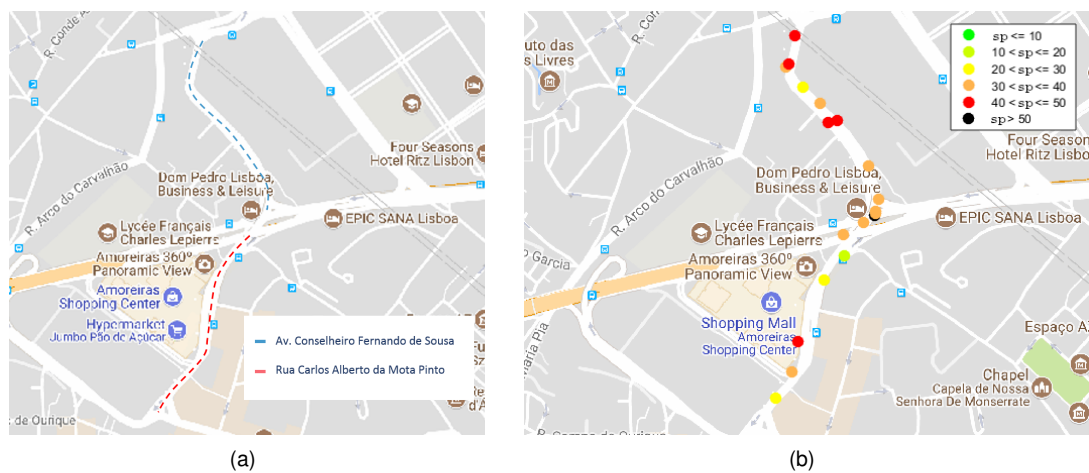


**Figure 4.5:** Representation of all overtaking maneuvers detected in several trips in 2 specific streets. (a) Avenida Conselheiro Fernando de Sousa and Rua Carlos Alberto da Mota Pinto highlighted; (b) Georeference results.

### Area C: Avenida 5 de Outubro and Avenida António Serpa

This two streets, represented in Fig.4.6 give access to main streets with large traffic flow along the day. Although Av. António Serpa have been recently changed to a mixed traffic road, in which a cycle lane is integrated and a speed limit of 30 km/h is posted, 75% of the overtaking maneuvers exceeded 30 km/h. In the other hand, in Av. 5 de Outubro 69.23% of overtaking maneuvers occurred at less than 30 km/h.

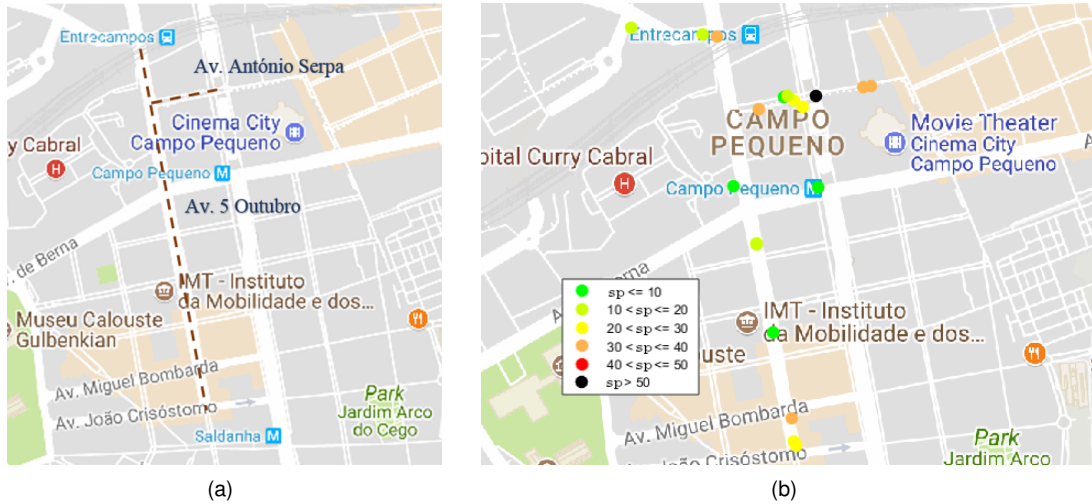


**Figure 4.6:** Representation of all overtaking maneuvers detected in several trips in 2 specific streets. (a) Av. António Serpa and Av. 5 de Outubro highlighted; (b) Georeference results.

### Area F: Avenida Almirante Reis

In Avenida Almirante Reis 25% of the total number of overtaking maneuvers were identified, proving that this main street has an increased traffic flow compared with other as Area A, where only 6.67% of the total number of overtaking maneuvers were identified. Concerning speed, the results prove to be inconclusive since the values spread equally for all intervals, which suggest that new sections could be considered. The overall results obtained for each street concerning overtaking maneuvers speed are presented in Table. 4.3.



**Figure 4.7:** Representation of all overtaking maneuvers detected in several trips in a specific section of a street (Av. Alm. Reis). (a) Av. Almirante Reis highlighted; (b) Georeference results.

**Table 4.3:** Overtaking maneuvers detections results. Street and speed range specification.

Streets	Speed (sp)			
	$sp \leq 20$	$20 < sp \leq 30$	$30 < sp \leq 40$	$sp > 40$
Campo de Ourique	59.09%	18.18%	13.64%	9.09%
Av. Conselheiro Fernando de Sousa	0	6.67%	53.33%	40%
Rua Carlos Alberto da Mota Pinto	7.14%	42.86%	35.71%	14.29%
Av. 5 de Outubro	53.85%	15.38%	30.77%	0
Av. António Serpa	25%	0	50%	25%
Av. Almirante de Reis	24.36%	15.38%	24.36%	35.90%

# Chapter 5

## Conclusions

### 5.1 Conclusions

A new method for speed estimation is proposed in this work, based on license plate detection and tracking, in order to identify and classify overtaking maneuvers performed by vehicles in the cyclists' surroundings. A method to estimate overtaking maneuvers speed has been presented, together with an occurrences map creation, providing a framework for later path characterization concerning bicycles' suitability and safety.

Furthermore, the proposed approach is suitable for implementation in real time systems, through an adaptation of detection module that requires an off line process for the presented approach. The results achieved can be used to complement existing approaches to assess risk of approaching vehicles as in [15] and alert the drivers, contribute to path characterization, as in ([1] and [2]), and provide useful information for classifying roads concerning bicycle suitability accordingly to the criteria mentioned in Table B.3.

It was possible to distinguish different urban areas based on the speed of detected overtaking maneuvers. Besides this, the results obtained matched the expected results, based on static classification of specific urban areas, concerning traffic flow and speed limits. It was possible to characterize calm neighborhoods ( area A and G) where at least 60% of detected overtaking maneuvers were performed under 20 km/h, to more requested areas, where almost 60% of overtaking maneuvers were detected with speed values above 30 km/h.

The developed method works with independent modules, which represents an advantage since different strategies can be considered to each module in order to improve results.

### 5.2 Future Work

In this problem context, Portuguese's license plate were being identified as generic European license plate. Character recognition module could be adapt to identify sequences of symbols with a known structure, or other approaches could be applied, focus on specific features to more complex methods.

License Plate recognition performance depends heavily on lightning conditions and poor image quality, caused by the natural trepidation caused by bicycle movement. An improved mechanism to hold the camera could be considered in order to acquire more data and achieve more robust results, once speed estimation is based on the coordinates of detected license plates, which if not correctly estimated could lead to incorrect speed estimation measurements.

The proposed approach can be improved by defining new sets of parameters to handle more specific events, such as bicycle overtaking moving cars, which represent an important information to characterize roads concerning traffic flow. It would also be worthwhile to identify parking areas, which may influence the bicycle suitability of a road. Besides the detailed approach, collecting more data in different areas at different hours of the day using cyclists with different experience would provide a more complete data set.

# Bibliography

- [1] P. Vieira, J. P. Costeira, S. Brandao, and M. Marques. SMARTcycling: Assessing cyclists' driving experience. *IEEE Intelligent Vehicles Symposium, Proceedings*, 2016.
- [2] M. Costa, B. Q. Ferreira, and M. Marques. A context aware and video-based risk descriptor for cyclists. In *IEEE Int. Conf. on Intelligent Transportation Systems*, 2017.
- [3] B. Blanc and M. Figliozzi. Modeling the impacts of facility type, trip characteristics, and trip stressors on cyclists' comfort levels utilizing crowdsourced data. *Transportation Research Record: Journal of the Transportation Research Board*, 2015.
- [4] J. Zacharias and R. Zhang. Revealed bicyclist route preferences and street conditions. *Transportation Research Record: Journal of the Transportation Research Board*, 2016.
- [5] Transportation Research Board. *2010 Highway Capacity Manual*. 2011.
- [6] M. B. Lowry, D. Callister, M. Gresham, and B. Moore. Using Bicycle Level of Service to Assess Community-wide Bikeability. *Transportation Research Record, Journal of the Transportation Research Board*, 2012.
- [7] San Francisco Department of Public Health. Bicycle Environmental Quality Index (BEQI). Technical report, 2009.
- [8] R. Doorley, V. Pakrashi, E. Byrne, S. Comerford, B. Ghosh, and J. A. Groeger. Analysis of heart rate variability amongst cyclists under perceived variations of risk exposure. *Transportation Research Part F: Traffic Psychology and Behaviour*, 2015.
- [9] J. Emery, C. Crump, and P. Bors. Reliability and Validity of Two Instruments Suitability of Sidewalks and Roads. *American Journal of Health Promotion*, 2003.
- [10] Bellevue Transportation Commission. MMLOS Metrics, Standards & Guidelines. Technical report, 2017.
- [11] Department for Transport. "Road accidents and safety statistics". <https://www.gov.uk/government/collections/road-accidents-and-safety-statistics>, 2016. [Online; accessed 04-July-2017].

- [12] RoSPA, The Royal Society for the Prevention of Accidents. "Cycling Accidents" . <https://www.gov.uk/government/collections/road-accidents-and-safety-statistics>, 2015. [Online; accessed 04-July-2017].
- [13] ANSR, Autoridade Nacional Segurança Rodoviária. "Principais Indicadores de Sinistralidade Continental". <http://www.ansr.pt/Estatisticas/RelatoriosDeSinistralidade/Documents/2016/RELAT>, 2016. [Online; accessed 04-July-2017].
- [14] Toronto cycling app. <https://www.toronto.ca/services-payments/streets-parking-transportation/cycling-in-toronto/toronto-cycling-app/>. [Online; accessed 20-April-2018].
- [15] C. Tonde and L. Iftode. *The Cyber-Physical Bike: A Step Towards Safer Green Transportation*. 2010.
- [16] M. Dozza and P. Gustafsson. *BikeCOM – A cooperative safety application supporting cyclists and drivers at intersections. Proceedings of the 3rd Conference of Driver Distraction and Inattention, Gothenbrug*, 2013.
- [17] C. Pinart, J. C. Calvo, L. Nicholson, and J. A. Villaverde. *ECall-compliant early crash notification service for portable and nomadic devices. IEEE Vehicular Technology Conference*, 2009.
- [18] D. A. Johnson and M. M. Trivedi. Driving style recognition using a smartphone as a sensor platform. In *2011 14th International IEEE Conference on Intelligent Transportation Systems (ITSC)*, 2011.
- [19] H. Eren, S. Makinist, E. Akin, and A. Yilmaz. Estimating driving behavior by a smartphone. In *2012 IEEE Intelligent Vehicles Symposium*, 2012.
- [20] H. Malik and A. Rakotonirainy. The need of intelligent driver training systems for road safety. In *Proceedings of 19th International Conference on Systems Engineering, ICSEng 2008*, 2008.
- [21] M. Lan, M. Rofouei, S. Soatto, and M. Sarrafzadeh. Smartldws: A robust and scalable lane departure warning system for the smartphones. In *2009 12th International IEEE Conference on Intelligent Transportation Systems*, 2009.
- [22] N. A. Mandellos, I. Keramitsoglou, and C. T. Kiranoudis. A background subtraction algorithm for detecting and tracking vehicles. *Expert Systems with Applications*, 2011.
- [23] C. C. R. Wang and J. J. J. Lien. Automatic vehicle detection using local features;a statistical approach. *IEEE Transactions on Intelligent Transportation Systems*, 2008.
- [24] Y. Zhao, J. Gu, C. Liu, S. Han, Y. Gao, and Q. Hu. License plate location based on haar-like cascade classifiers and edges. In *2010 Second WRI Global Congress on Intelligent Systems*, 2010.
- [25] P. K. Bhaskar and S. P. Yong. Image processing based vehicle detection and tracking method. In *2014 International Conference on Computer and Information Sciences (ICCOINS)*, 2014.
- [26] A. Geiger, P. Lenz, and R. Urtasun. *Are we ready for Autonomous Driving? The KITTI Vision Benchmark Suite. Computer Vision and Pattern Recognition*, 2012.

- [27] C. Maduro, K. Batista, P. Peixoto, and J. Batista. Estimation of vehicle velocity and traffic intensity using rectified images. *Proceedings - International Conference on Image Processing, ICIP*, 2008.
- [28] M. S. Temiz, S. Kulur, and S. Dogan. Real Time Speed Estimation From Monocular Video. *ISPRS - International Archives of the Photogrammetry, Remote Sensing and Spatial Information Sciences*, 2012.
- [29] T. Celik and H. Kusetogullari. Solar-powered automated road surveillance system for speed violation detection. *IEEE Transactions on Industrial Electronics*, 2010.
- [30] M. Kampelmühler, M. G. Müller, and C. Feichtenhofer. Camera-based vehicle velocity estimation from monocular video. *CoRR*, 2018.
- [31] S. L. Chang, L. S. Chen, Y. C. Chung, and S. W. Chen. Automatic License Plate Recognition. *IEEE Transactions on Intelligent Transportation Systems*, 2004.
- [32] T. D. Duan, D. A. Duc, and T. L. H. Du. Combining Hough transform and contour algorithm for detecting vehicles' license-plates. *Proceedings of 2004 International Symposium on Intelligent Multimedia, Video and Speech Processing.*, 2004.
- [33] D. Mitra, S. Banerjee, and A. Kalam. Automatic number plate recognition system: A histogram based approach. 2016.
- [34] H. Caner, H. S. Gecim, and A. Z. Alkar. Efficient embedded neural-network-based license plate recognition system. *IEEE Transactions on Vehicular Technology*, 2008.
- [35] T. Björklund. Automatic License Plate Recognition with Convolutional Neural Networks Trained on Synthetic Data. 2017.
- [36] Openalpr - automatic license plate recognition. <http://www.openalpr.com/>. [Online; accessed 21-March-2018].
- [37] H. N. Do, M. T. Vo, B. Q. Vuong, H. T. Pham, A. H. Nguyen, and H. Q. Luong. Automatic license plate recognition using mobile device. In *2016 International Conference on Advanced Technologies for Communications (ATC)*, 2016.
- [38] R. Mithe, S. Indalkar, and N. Divekar. Optical Character Recognition. *International Journal of Recent Technology and Engineering (IJRTE)*, 2013.
- [39] T. Ojala, M. Pietikainen, and T. Maenpaa. Multiresolution gray-scale and rotation invariant texture classification with local binary patterns. *IEEE Transactions on Pattern Analysis and Machine Intelligence*, 2002.
- [40] A. Schrijver. *Theory of Linear and Integer Programming*. John Wiley & Sons, Inc., New York, NY, USA, 1986.

- [41] Câmara Municipal de Lisboa . "Mobilidade Ciclável". <http://www.cm-lisboa.pt/viver/mobilidade/mobilidade-ciclavel/rede-ciclavel>, 2018. [Online; accessed 10-May-2018].
- [42] J. Davis. Bicycle Safety Evaluation. Technical report, Auburn University, City of Chattanooga, and Chattanooga-Hamilton County Regional Planning Commission, Chattanooga, 1987.
- [43] A. Sorton and T. Walsh. Bicycle stress level as a tool to evaluate urban and suburban bicycle compatibility. *Transportation Research Record: Journal of the Transportation Research Board*, 1994.
- [44] B. Epperson. Evaluating suitability of roadways for bicycle use: Toward a cycling level-of-service standard. *Transportation Research Record: Journal of the Transportation Research Board*, 1994.
- [45] B. W. Landis. Bicycle Interaction Hazard Score: a Theoretical Model. *Transportation Research Record: Journal of the Transportation Research Board*, 1994.
- [46] Federal Highway Administration. Development of the Bicycle Compability Index: a level of Service Concept. Technical report, 1998.
- [47] M. C. Mekuria, P. G. Furth, and H. Nixon. Low-Stress Bicycling and Network Connectivity Low-Stress Bicycling and Network Connectivity. *Transportation Commons*, 2012.
- [48] Transportation Research Board. Highway Capacity Manual. 2017.

# Appendix A

## Figures

### A.1 Overtaking Maneuvers Identification

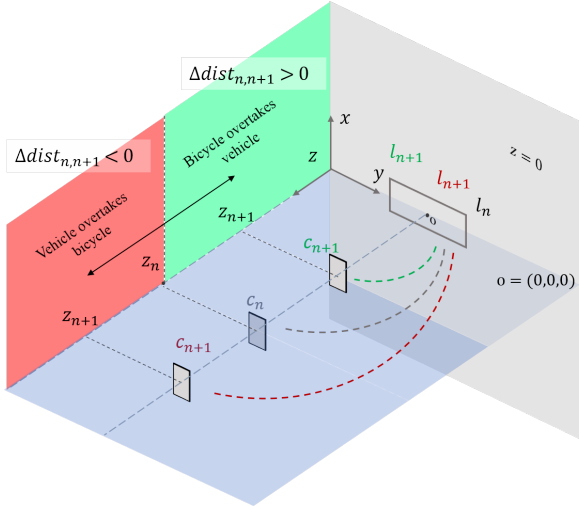


**Figure A.1:** Distance measurement between two detections,  $l_n$  and  $l_{n+1}$  represent two license plates detected at different instances of time. Vehicle performing an overtaking maneuver,  $z_{n+1} > z_n$ ; Cyclist performing an overtaking maneuver,  $z_{n+1} < z_n$ .

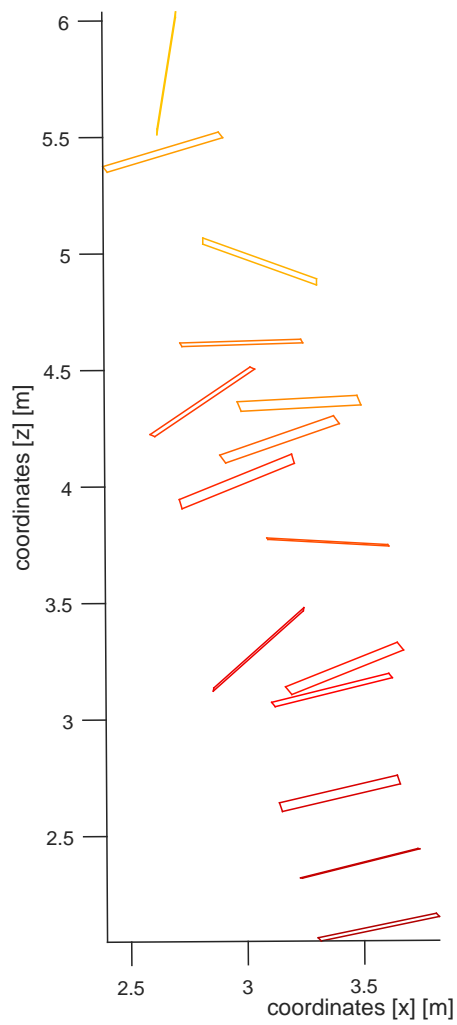


**Figure A.2:** 3D Representation of all detections of a vehicle performing an overtaking maneuver.

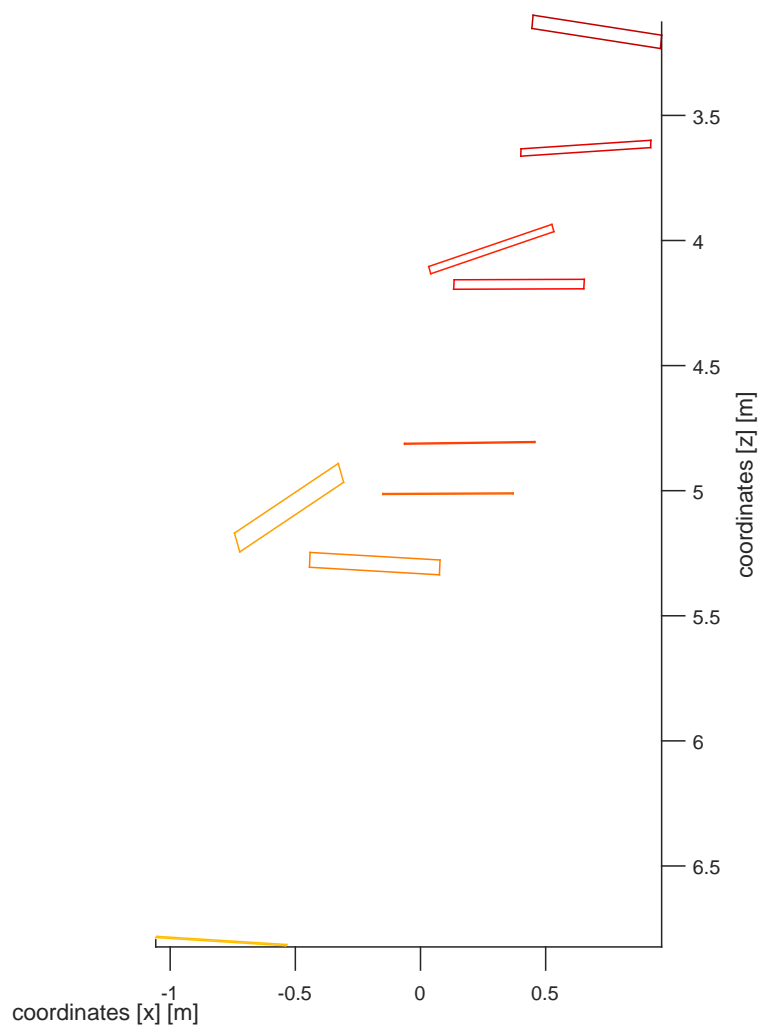


**Figure A.3:** 3D Representation of all detections to a parked vehicle.



# Appendix B

## Tables

### B.1 Streets Characterization

**Table B.1:** Bicycle suitability methods, acronym, reference, citation and date.

Method	Acronym	Reference	Date
Bicycle safety index rate	BSIR	Davis [42]	1987
Bicycle Stress Level	BSI	Sorton and Walsh [43]	1994
Road Condition Index	RCI	Epperson [44]	1994
Interaction Hazard Score	IHS	Landis [45]	1994
Bicycle Compatibility Index	BCI	Harkey et al [46]	1998
Bicycle Suitability Assessment	BSA	Emery and Crump [9]	2003
Bicycle Environmental Quality index	BEQI	Fehr and Peers [7]	2009
Bicycle Level of Stress	BLOS	HCM2010 [5]	2010
Level of traffic stress	LTS	Mekuria [47]	2012
Multi-modal Level of Service	MMLOS	HCM6 [48]	2017

**Table B.2:** Side-by-side comparison of considered variables on listed methods.

Variables	Method, data	BSIR, 1987	BSL, 1994	RCI, 1994	IHS, 1994	BCI, 1998	BSA, 2003	BEQI, 2009	BLOS, 2010	LTS, 2012	MMLOS, 2017
Vehicle speed		x	x	x	x	x	x	x	x	x	x
Vehicle traffic volume		x	x	x	x	x	x	x	x	x	x
Number of traffic lanes		x			x	x	x	x	x	x	
Speed limit		x								x	
Width of outside traffic lanes		x			x		x		x	x	x
Width of bicycle lane		x	x	x	x	x	x	x			
Width of roadside		x	x						x		
Pavement factors		x		x	x	x	x	x		x	x
Signalization factors		x						x			x
Presence of bicycle lane				x		x	x	x	x	x	x
Percent of heavy vehicles				x	x	x		x	x		x
Parking on the lane				x	x	x	x	x	x	x	
Curb/physical separation			x			x	x		x	x	x
Slope							x	x			x
Turning lane							x				
Frequent curves									x		
Field of view		x		x				x			
Lane blockage											x

**Table B.3:** Specific streets characterization.

Street Name	Feature	Area	Number of lanes	Speed limit [km/h]	Parking areas	Intersections	Roundabouts
Av. António Serpa		C	2	30	Yes	Yes	No
Av. 5 de Outubro		C	2	50	Yes	Yes	No
Av. Almirante de Reis		E	2	50	Yes	Yes	No
Av. Conselheiro Fernando de Sousa		B	3	50	Yes	Yes	No
Rua Carlos Alberto da Mota Pinto		B	2	50	No	Yes	No
Av. Afonso Costa		F	3-4	50	No	No	Yes

